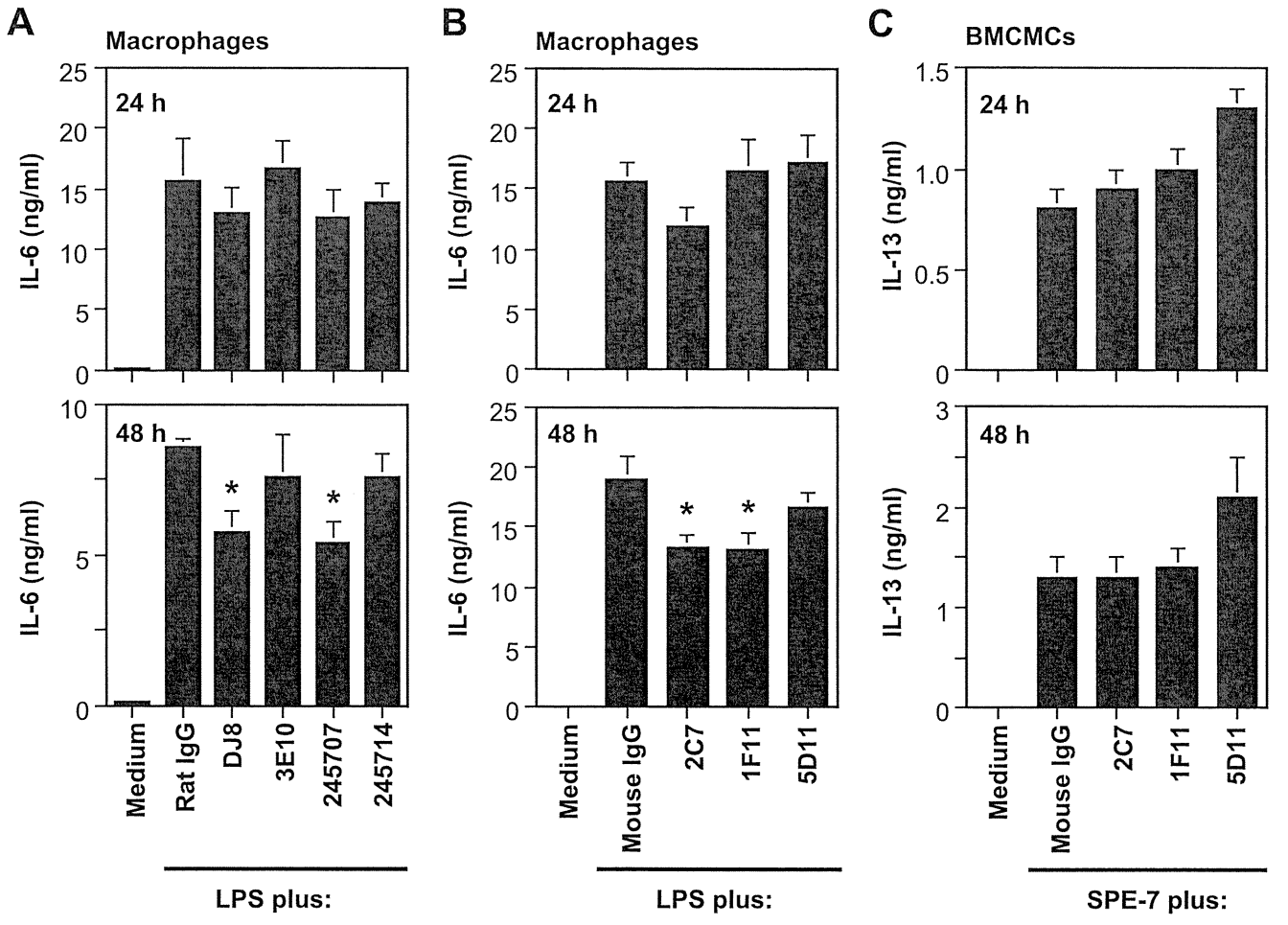

Figure 5. Inhibitory effects of anti-IL-33 mAbs on LPS-mediated macrophage activation by paracrine IL-33 stimulation. (A, B) TGC-induced peritoneal macrophages derived from B6J-WT mice were cultured in the presence of 100 ng/ml LPS, with and without 40 μg/ml of several anti-ST2 mAbs (A), several anti-IL-33 mAbs (B) or control IgG (A, B) for 24 and 48 h. (C) B6J-WT BMCMCs were cultured in the presence of 1 μg/ml anti-DNP IgE (SPE-7), with and without 40 μg/ml of several anti-IL-33 mAbs or control IgG for 24 and 48 h. The levels of IL-6 or IL-13 in the culture supernatants were measured by ELISA. Data show the mean + SEM ([A] n = 7, [B] n = 8 [C] n = 4). *$p<0.05$ vs. Rat IgG (A) or Mouse IgG (B).
doi:10.1371/journal.pone.0018404.g005

Discussion

Like ST2$^{-/-}$ mice [56] and mice treated with a soluble ST2-Fc fusion protein [57], mice treated with a certain anti-ST2 mAb (generated by Amgen) showed attenuated development of collagen-induced arthritis [58]. Since that ST2 mAb (Amgen) inhibited IL-33-mediated immune responses *in vitro* and *in vivo*, it is considered to act as a blocking Ab for binding of IL-33 to ST2. Conversely, mice treated with an anti-ST2 polyclonal Ab showed aggravated development of collagen-induced arthritis [52]. Since that polyclonal Ab lysed ST2-expressing cells *in vitro*, its *in vivo* administration may have depleted certain ST2-expressing regulatory cells such as Tr1 cells [59] as well as ST2-expressing effector cells such as mast cells [56], thereby causing aggravation, rather than attenuation, of the arthritis. However, the precise activities (i.e., depletion, agonism, blocking, etc.) of the other ST2 Abs were poorly characterized in the previous studies, because many of which were performed before the identification of IL-33.

It is well known that the biological activities of the IL-1 family of cytokines are elaborately regulated by decoy/soluble receptors, binding proteins and/or receptor antagonists [60,61]. For example, the activities of IL-1α and IL-1β are mediated by IL-1R (IL-1R1 and IL-1RAcP), but blocked by IL-1R2, the soluble form IL-1Rs and IL-1 receptor antagonist (IL-1Ra) [60,61]. The activities of IL-18 are mediated by IL-18R, but inhibited by IL-18-binding protein [60,61]. On the other hand, inconsistent results were reported between a ligand- and its receptor-deficient mice even on the same genetic background. For example, experimental autoimmune encephalomyelitis developed normally in IL-18$^{-/-}$ mice, but not in IL-18Rα$^{-/-}$ mice [62]. These observations suggest involvement of another ligand(s) besides IL-18, i.e., IL-1F7 [63], in the development of the disease. Moreover, IL-1F10, in addition to IL-1α, IL-1β and IL-1Ra, also can bind to IL-1R1, although its binding affinity is low compared with IL-1β and IL-1Ra [64]. Therefore, like IL-18Rα and IL-1R1, ST2 may be a component of receptors for another ligand(s) besides IL-33. As another possibility, IL-33 may bind to other receptors besides ST2, SIGIRR/Tir8 [65] and c-Kit [66]. Thus, it was surmised that, for elucidation of the precise roles of IL-33 *in vivo* and *in vitro*, it would be more advantageous to use neutralizing Abs for IL-33 rather than for ST2. Therefore, in the present study, we newly generated anti-IL-33 mAbs and characterized their functions as well as the functions of anti-ST2 Abs.

We and the others have shown that macrophages can release IL-33 after LPS stimulation [44], and IL-33 can enhance LPS-mediated TNF and IL-6 production by macrophages (Fig. 4A)

[43]. We also found that IL-33$^{-/-}$ macrophages showed reduced IL-6 production in response to LPS (Fig. 4C). Likewise, LPS-mediated IL-6 production by macrophages was inhibited by treatment with anti-IL-33 mAbs (2C7 and 1F11, but not other mAbs) (Fig. 5B and data not shown), a soluble ST2-Fc fusion protein [15] or anti-ST2 mAbs (DJ8 and 245707, but not 3E10 and 245714) (Fig. 5A). It was reported that IL-1, IL-6, IL-12 and TNF production by macrophages from ST2$^{-/-}$ mice on the BALB/c background was increased [16] or comparable [43] with those from wild-type mice at 12, 24 or 48 h after LPS stimulation. The apparent discrepancy between ST2$^{-/-}$ macrophages and IL-33$^{-/-}$/anti-ST2 mAb-treated/soluble ST2-Fc fusion protein-treated macrophages may be accounted for as described elsewhere [4]. Nonetheless, these observations (except the study using ST2$^{-/-}$ macrophages [16]) suggest that macrophages produce IL-33 in response to LPS, and that that IL-33 then additively promotes LPS-mediated macrophage activation.

The inhibitory levels of cytokine production by macrophages treated with anti-IL-33 neutralizing Ab was lesser than those by IL-33$^{-/-}$ macrophages after LPS stimulation. It is considered that IL-33 has dual roles as a cytokine and a nuclear factor [67,68,69]. The function of both secreted and nuclear IL-33 was abrogated in IL-33-deficient cells. On the other hand, the neutralizing antibody for IL-33 and/or ST2 can inhibit the effect of secreted IL-33, but not that of nuclear IL-33. Thus, the difference between anti-IL-33 neutralizing antibody-treated and IL-33-deficient macrophages may be due to the potential role of IL-33 in the nucleus.

Anti-IL-33 mAb 5D11 inhibited recombinant IL-33$_{109-266}$-dependent IL-13 production by BMCMCs (Fig. 3B). Conversely, it did not inhibit the activity of endogenous IL-33 (probably full-length IL-33) in LPS-mediated IL-6 production by macrophages (Fig. 5B). Like anti-IL-33 mAb Nessy-1, our anti-IL-33 mAbs were generated against IL-33$_{109-266}$, not full-length IL-33, and it seemed that some of them including 1D2, 2A2, and 2E6 could not inhibit the activities of full-length IL-33 even though they neutralized recombinant IL-33$_{109-266}$ (Fig. 3B and data not shown).

In conclusion, our findings suggest that IL-33-neutralizing mAbs, which we newly generated, will be useful tools for the understanding the pathophysiological function(s) of IL-33 *in vitro* and presumably *in vivo*. They also have potential for aiding in the development of new therapeutics for certain IL-33-mediated disorders.

Acknowledgments

We thank Drs. Tsuneyasu Kaisyo and (RIKEN, Japan) and Andrew N.J. McKenzie (MRC, Cambridge, UK) for providing B6J-TLR4$^{-/-}$ mice and BALB-ST2$^{-/-}$ mice, and Michiko Yamada, Hiromi Wakita, Shuhei Fukuda and Noriko Hashimoto for their excellent technical assistance.

Author Contributions

Analyzed the data: TO K. Oboki KA HM NK. Contributed reagents/materials/analysis tools: M. Iikura TA JI KM KS MA K. Okumura TK HS. Wrote the paper: TO K. Oboki SN. Designed the study: TO K. Oboki SN. Performed the research: TO K. Oboki KA HM NK. Generation of anti-IL-33 mAbs: ST M. Ikeda.

References

1. Schmitz J, Owyang A, Oldham E, Song Y, Murphy E, et al. (2005) IL-33, an interleukin-1-like cytokine that signals via the IL-1 receptor-related protein ST2 and induces T helper type 2-associated cytokines. Immunity 23: 479–490.
2. Smith DE (2010) IL-33: a tissue derived cytokine pathway involved in allergic inflammation and asthma. Clin Exp Allergy 40: 200–208.
3. Liew FY, Pitman NI, McInnes IB (2010) Disease-associated functions of IL-33: the new kid in the IL-1 family. Nat Rev Immunol 10: 103–110.
4. Oboki K, Ohno T, Kajiwara N, Saito H, Nakae S (2010) IL-33 and IL-33 receptors in host defense and diseases. Allergol Int 59: 143–160.
5. Chackerian AA, Oldham ER, Murphy EE, Schmitz J, Pflanz S, et al. (2007) IL-1 receptor accessory protein and ST2 comprise the IL-33 receptor complex. J Immunol 179: 2551–2555.
6. Cherry WB, Yoon J, Bartemes KR, Iijima K, Kita H (2008) A novel IL-1 family cytokine, IL-33, potently activates human eosinophils. J Allergy Clin Immunol 121: 1484–1490.
7. Ho LH, Ohno T, Oboki K, Kajiwara N, Suto H, et al. (2007) IL-33 induces IL-13 production by mouse mast cells independently of IgE-FcepsilonRI signals. J Leukoc Biol 82: 1481–1490.
8. Moulin D, Donze O, Talabot-Ayer D, Mezin F, Palmer G, et al. (2007) Interleukin (IL)-33 induces the release of pro-inflammatory mediators by mast cells. Cytokine 40: 216–225.
9. Iikura M, Suto H, Kajiwara N, Oboki K, Ohno T, et al. (2007) IL-33 can promote survival, adhesion and cytokine production in human mast cells. Lab Invest 87: 971–978.
10. Allakhverdi Z, Smith DE, Comeau MR, Delespesse G (2007) The ST2 ligand IL-33 potently activates and drives maturation of human mast cells. J Immunol 179: 2051–2054.
11. Ali S, Huber M, Kollewe C, Bischoff SC, Falk W, et al. (2007) IL-1 receptor accessory protein is essential for IL-33-induced activation of T lymphocytes and mast cells. Proc Natl Acad Sci U S A 104: 18660–18665.
12. Suzukawa M, Iikura M, Koketsu R, Nagase H, Tamura C, et al. (2008) An IL-1 cytokine member, IL-33, induces human basophil activation via its ST2 receptor. J Immunol 181: 5981–5989.
13. Pecaric-Petkovic T, Didichenko SA, Kaempfer S, Spiegl N, Dahinden CA (2009) Human basophils and eosinophils are the direct target leukocytes of the novel IL-1 family member IL-33. Blood 113: 1526–1534.
14. Kondo Y, Yoshimoto T, Yasuda K, Futatsugi-Yumikura S, Morimoto M, et al. (2008) Administration of IL-33 induces airway hyperresponsiveness and goblet cell hyperplasia in the lungs in the absence of adaptive immune system. Int Immunol 20: 791–800.
15. Sweet MJ, Leung BP, Kang D, Sogaard M, Schulz K, et al. (2001) A novel pathway regulating lipopolysaccharide-induced shock by ST2/T1 via inhibition of Toll-like receptor 4 expression. J Immunol 166: 6633–6639.
16. Brint EK, Xu D, Liu H, Dunne A, McKenzie AN, et al. (2004) ST2 is an inhibitor of interleukin 1 receptor and Toll-like receptor 4 signaling and maintains endotoxin tolerance. Nat Immunol 5: 373–379.
17. Allakhverdi Z, Comeau MR, Smith DE, Toy D, Endam LM, et al. (2009) CD34^{+} hemopoietic progenitor cells are potent effectors of allergic inflammation. J Allergy Clin Immunol 123: 472–478.
18. Moro K, Yamada T, Tanabe M, Takeuchi T, Ikawa T, et al. (2010) Innate production of T(H)2 cytokines by adipose tissue-associated c-Kit^{+}Sca-1^{+} lymphoid cells. Nature 463: 540–544.
19. Neill DR, Wong SH, Bellosi A, Flynn RJ, Daly M, et al. (2010) Nuocytes represent a new innate effector leukocyte that mediates type-2 immunity. Nature 464: 1367–1370.
20. Gudbjartsson DF, Bjornsdottir US, Halapi E, Helgadottir A, Sulem P, et al. (2009) Sequence variants affecting eosinophil numbers associate with asthma and myocardial infarction. Nat Genet 41: 342–347.
21. Reijmerink NE, Postma DS, Bruinenberg M, Nolte IM, Meyers DA, et al. (2008) Association of IL1RL1, IL18R1, and IL18RAP gene cluster polymorphisms with asthma and atopy. J Allergy Clin Immunol 122: 651–654 e658.
22. Ali M, Zhang G, Thomas WR, McLean CJ, Bizzintino JA, et al. (2009) Investigations into the role of ST2 in acute asthma in children. Tissue Antigens 73: 206–212.
23. Shimizu M, Matsuda A, Yanagisawa K, Hirota T, Akahoshi M, et al. (2005) Functional SNPs in the distal promoter of the ST2 gene are associated with atopic dermatitis. Hum Mol Genet 14: 2919–2927.
24. Sakashita M, Yoshimoto T, Hirota T, Harada M, Okubo K, et al. (2008) Association of serum interleukin-33 level and the interleukin-33 genetic variant with Japanese cedar pollinosis. Clin Exp Allergy 38: 1875–1881.
25. Castano R, Bosse Y, Endam LM, Desrosiers M (2009) Evidence of association of interleukin-1 receptor-like 1 gene polymorphisms with chronic rhinosinusitis. Am J Rhinol Allergy 23: 377–384.
26. Smithgall MD, Comeau MR, Yoon BR, Kaufman D, Armitage R, et al. (2008) IL-33 amplifies both Th1- and Th2-type responses through its activity on human basophils, allergen-reactive Th2 cells, iNKT and NK cells. Int Immunol 20: 1019–1030.
27. Kurowska-Stolarska M, Stolarski B, Kewin P, Murphy G, Corrigan CJ, et al. (2009) IL-33 amplifies the polarization of alternatively activated macrophages that contribute to airway inflammation. J Immunol 183: 6469–6477.
28. Kuroiwa K, Li H, Tago K, Iwahana H, Yanagisawa K, et al. (2000) Construction of ELISA system to quantify human ST2 protein in sera of patients. Hybridoma 19: 151–159.
29. Oshikawa K, Kuroiwa K, Tago K, Iwahana H, Yanagisawa K, et al. (2001) Elevated soluble ST2 protein levels in sera of patients with asthma with an acute exacerbation. Am J Respir Crit Care Med 164: 277–281.

30. Prefontaine D, Lajoie-Kadoch S, Foley S, Audusseau S, Olivenstein R, et al. (2009) Increased expression of IL-33 in severe asthma: evidence of expression by airway smooth muscle cells. J Immunol 183: 5094–5103.
31. Matsuda A, Okayama Y, Terai N, Yokoi N, Ebihara N, et al. (2009) The role of interleukin-33 in chronic allergic conjunctivitis. Invest Ophthalmol Vis Sci 50: 4646–4652.
32. Pushparaj PN, Tay HK, H'Ng SC, Pitman N, Xu D, et al. (2009) The cytokine interleukin-33 mediates anaphylactic shock. Proc Natl Acad Sci U S A 106: 9773–9778.
33. Hoshino K, Kashiwamura S, Kuribayashi K, Kodama T, Tsujimura T, et al. (1999) The absence of interleukin 1 receptor-related T1/ST2 does not affect T helper cell type 2 development and its effector function. J Exp Med 190: 1541–1548.
34. Mangan NE, Dasvarma A, McKenzie AN, Fallon PG (2007) T1/ST2 expression on Th2 cells negatively regulates allergic pulmonary inflammation. Eur J Immunol 37: 1302–1312.
35. Kurowska-Stolarska M, Kewin P, Murphy G, Russo RC, Stolarski B, et al. (2008) IL-33 induces antigen-specific IL-5$^+$ T cells and promotes allergic-induced airway inflammation independent of IL-4. J Immunol 181: 4780–4790.
36. Meisel C, Bonhagen K, Lohning M, Coyle AJ, Gutierrez-Ramos JC, et al. (2001) Regulation and function of T1/ST2 expression on CD4$^+$ T cells: induction of type 2 cytokine production by T1/ST2 cross-linking. J Immunol 166: 3143–3150.
37. Kearley J, Buckland KF, Mathie SA, Lloyd CM (2009) Resolution of allergic inflammation and airway hyperreactivity is dependent upon disruption of the T1/ST2-IL-33 pathway. Am J Respir Crit Care Med 179: 772–781.
38. Coyle AJ, Lloyd C, Tian J, Nguyen T, Erikkson C, et al. (1999) Crucial role of the interleukin 1 receptor family member T1/ST2 in T helper cell type 2-mediated lung mucosal immune responses. J Exp Med 190: 895–902.
39. Oshikawa K, Yanagisawa K, Tominaga S, Sugiyama Y (2002) Expression and function of the ST2 gene in a murine model of allergic airway inflammation. Clin Exp Allergy 32: 1520–1526.
40. Lohning M, Stroehmann A, Coyle AJ, Grogan JL, Lin S, et al. (1998) T1/ST2 is preferentially expressed on murine Th2 cells, independent of interleukin 4, interleukin 5, and interleukin 10, and important for Th2 effector function. Proc Natl Acad Sci U S A 95: 6930–6935.
41. Culley FJ (2009) Natural killer cells in infection and inflammation of the lung. Immunology 128: 151–163.
42. Umetsu DT, DeKruyff RH (2006) A role for natural killer T cells in asthma. Nat Rev Immunol 6: 953–958.
43. Espinassous Q, Garcia-de-Paco E, Garcia-Verdugo I, Synguelakis M, von Aulock S, et al. (2009) IL-33 enhances lipopolysaccharide-induced inflammatory cytokine production from mouse macrophages by regulating lipopolysaccharide receptor complex. J Immunol 183: 1446–1455.
44. Ohno T, Oboki K, Kajiwara N, Morii E, Aozasa K, et al. (2009) Caspase-1, caspase-8, and calpain are dispensable for IL-33 release by macrophages. J Immunol 183: 7890–7897.
45. Hoshino K, Takeuchi O, Kawai T, Sanjo H, Ogawa T, et al. (1999) Cutting edge: Toll-like receptor 4 (TLR4)-deficient mice are hyporesponsive to lipopolysaccharide: evidence for TLR4 as the Lps gene product. J Immunol 162: 3749–3752.
46. Townsend MJ, Fallon PG, Matthews DJ, Jolin HE, McKenzie AN (2000) T1/ST2-deficient mice demonstrate the importance of T1/ST2 in developing primary T helper cell type 2 responses. J Exp Med 191: 1069–1076.
47. Naito A, Azuma S, Tanaka S, Miyazaki T, Takaki S, et al. (1999) Severe osteopetrosis, defective interleukin-1 signalling and lymph node organogenesis in TRAF6-deficient mice. Genes Cells 4: 353–362.
48. Oboki K, TOhno, NKajiwara, KArae K, HMorita, et al. (2010) IL-33 is a crucial amplifier of innate rather than acquired immunity. Proc Natl Acad Sci U S A 107: 18581–18586.
49. Moritz DR, Gheyselinck J, Klemenz R (1998) Expression analysis of the soluble and membrane-associated forms of the interleukin-1 receptor-related T1 protein in primary mast cells and fibroblasts. Hybridoma 17: 107–116.
50. Moritz DR, Rodewald HR, Gheyselinck J, Klemenz R (1998) The IL-1 receptor-related T1 antigen is expressed on immature and mature mast cells and on fetal blood mast cell progenitors. J Immunol 161: 4866–4874.
51. Walzl G, Matthews S, Kendall S, Gutierrez-Ramos JC, Coyle AJ, et al. (2001) Inhibition of T1/ST2 during respiratory syncytial virus infection prevents T helper cell type 2 (Th2)- but not Th1-driven immunopathology. J Exp Med 193: 785–792.
52. Xu D, Chan WL, Leung BP, Huang F, Wheeler R, et al. (1998) Selective expression of a stable cell surface molecule on type 2 but not type 1 helper T cells. J Exp Med 187: 787–794.
53. Luthi AU, Cullen SP, McNeela EA, Duriez PJ, Afonina IS, et al. (2009) Suppression of interleukin-33 bioactivity through proteolysis by apoptotic caspases. Immunity 31: 84–98.
54. Cayrol C, Girard JP (2009) The IL-1-like cytokine IL-33 is inactivated after maturation by caspase-1. Proc Natl Acad Sci U S A 106: 9021–9026.
55. Kawakami T, Kitaura J, Xiao W, Kawakami Y (2005) IgE regulation of mast cell survival and function. Novartis Found Symp 271: 100–107. discussion 108–114, 145–151.
56. Xu D, Jiang HR, Kewin P, Li Y, Mu R, et al. (2008) IL-33 exacerbates antigen-induced arthritis by activating mast cells. Proc Natl Acad Sci U S A 105: 10913–10918.
57. Leung BP, Xu D, Culshaw S, McInnes IB, Liew FY (2004) A novel therapy of murine collagen-induced arthritis with soluble T1/ST2. J Immunol 173: 145–150.
58. Palmer G, Talabot-Ayer D, Lamacchia C, Toy D, Seemayer CA, et al. (2009) Inhibition of interleukin-33 signaling attenuates the severity of experimental arthritis. Arthritis Rheum 60: 738–749.
59. McGuirk P, McCann C, Mills KH (2002) Pathogen-specific T regulatory 1 cells induced in the respiratory tract by a bacterial molecule that stimulates interleukin 10 production by dendritic cells: a novel strategy for evasion of protective T helper type 1 responses by Bordetella pertussis. J Exp Med 195: 221–231.
60. Dinarello CA (2009) Immunological and inflammatory functions of the interleukin-1 family. Annu Rev Immunol 27: 519–550.
61. Sims JE, Smith DE (2010) The IL-1 family: regulators of immunity. Nat Rev Immunol 10: 89–102.
62. Gutcher I, Urich E, Wolter K, Prinz M, Becher B (2006) Interleukin 18-independent engagement of interleukin 18 receptor-α is required for autoimmune inflammation. Nat Immunol 7: 946–953.
63. Pan G, Risser P, Mao W, Baldwin DT, Zhong AW, et al. (2001) IL-1H, an interleukin 1-related protein that binds IL-18 receptor/IL-1Rrp. Cytokine 13: 1–7.
64. Lin H, Ho AS, Haley-Vicente D, Zhang J, Bernal-Fussell J, et al. (2001) Cloning and characterization of IL-1HY2, a novel interleukin-1 family member. J Biol Chem 276: 20597–20602.
65. Bulek K, Swaidani S, Qin J, Lu Y, Gulen MF, et al. (2009) The essential role of single Ig IL-1 receptor-related molecule/Toll IL-1R8 in regulation of Th2 immune response. J Immunol 182: 2601–2609.
66. Drube S, Heink S, Walter S, Lohn T, Grusser M, et al. (2010) The receptor tyrosine kinase c-Kit controls IL-33 receptor signaling in mast cells. Blood 115: 3899–3906.
67. Baekkevold ES, Roussigne M, Yamanaka T, Johansen FE, Jahnsen FL, et al. (2003) Molecular characterization of NF-HEV, a nuclear factor preferentially expressed in human high endothelial venules. Am J Pathol 163: 69–79.
68. Carriere V, Roussel L, Ortega N, Lacorre DA, Americh L, et al. (2007) IL-33, the IL-1-like cytokine ligand for ST2 receptor, is a chromatin-associated nuclear factor in vivo. Proc Natl Acad Sci U S A 104: 282–287.
69. Roussel L, Erard M, Cayrol C, Girard JP (2008) Molecular mimicry between IL-33 and KSHV for attachment to chromatin through the H2A-H2B acidic pocket. EMBO Rep 9: 1006–1012.

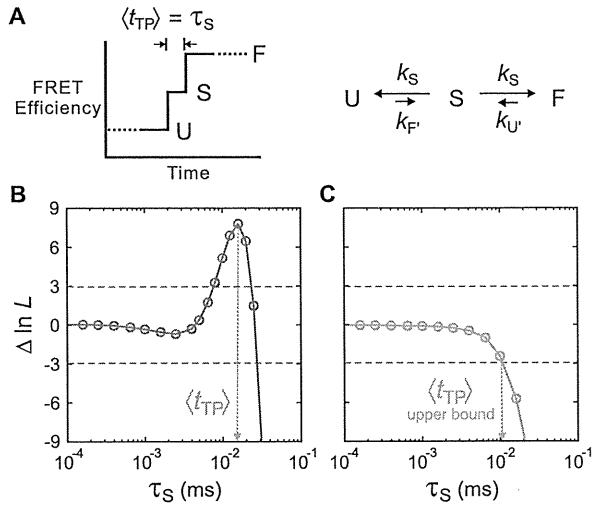

Fig. 4. Determination of average transition-path times in a kinetic model. **(A)** Schematic of a FRET efficiency trajectory using a one-step model to describe the transition path from unfolded (U) to folded (F) states for a protein exhibiting two-state kinetics and thermodynamics. The average transition-path time, $\langle t_{TP} \rangle$, is equal to the lifetime of a virtual intermediate state S [$\tau_S = (2k_S)^{-1}$]. (**B** and **C**) The difference of the log likelihood, $\Delta \ln L = \ln L(\tau_S) - \ln L(0)$, between the two-state model with a finite transition-path time and a two-state model with an instantaneous transition-path time is plotted as a function of τ_S (B) for the WW domain in 3 M GdmCl in 50% glycerol and (C) for protein GB1 in 4 M urea. The horizontal dashed line at $\Delta \ln L = +3$ represents the 95% confidence limit for the significance of the peak in (B), and the intersection of the likelihood function with the horizontal dashed line at $\Delta \ln L = -3$ in (C) yields the 95% confidence limit for the upper bound of τ_S.

is almost the same for two proteins with different topologies and vastly different folding rates.

References and Notes

1. J. D. Bryngelson, J. N. Onuchic, N. D. Socci, P. G. Wolynes, *Proteins* **21**, 167 (1995).
2. F. Noé, C. Schütte, E. Vanden-Eijnden, L. Reich, T. R. Weikl, *Proc. Natl. Acad. Sci. U.S.A.* **106**, 19011 (2009).
3. G. R. Bowman, V. S. Pande, *Proc. Natl. Acad. Sci. U.S.A.* **107**, 10890 (2010).
4. D. E. Shaw *et al.*, *Science* **330**, 341 (2010).
5. S. Piana, K. Lindorff-Larsen, D. E. Shaw, *Biophys. J.* **100**, L47 (2011).
6. K. Lindorff-Larsen, S. Piana, R. O. Dror, D. E. Shaw, *Science* **334**, 517 (2011).
7. H. Nguyen, M. Jager, A. Moretto, M. Gruebele, J. W. Kelly, *Proc. Natl. Acad. Sci. U.S.A.* **100**, 3948 (2003).
8. M. Petrovich, A. L. Jonsson, N. Ferguson, V. Daggett, A. R. Fersht, *J. Mol. Biol.* **360**, 865 (2006).
9. H. S. Chung, J. M. Louis, W. A. Eaton, *Proc. Natl. Acad. Sci. U.S.A.* **106**, 11837 (2009).
10. I. V. Gopich, A. Szabo, *J. Phys. Chem. B* **113**, 10965 (2009).
11. Materials and methods are available as supporting online material on *Science* Online.
12. G. Hummer, *J. Chem. Phys.* **120**, 516 (2004).
13. F. Liu, M. Nakaema, M. Gruebele, *J. Chem. Phys.* **131**, 195101 (2009).
14. I. C. Yeh, G. Hummer, *J. Phys. Chem. B* **108**, 15873 (2004).
15. N. D. Socci, J. N. Onuchic, P. G. Wolynes, *J. Chem. Phys.* **104**, 5860 (1996).
16. In the case of protein GB1, there is the possibility of a sparsely populated intermediate between the folded and unfolded states (*17–20*). In this study, we have implicitly defined the transition-path time for both the WW domain and protein GB1 in terms of just the two deep minima of the folded and unfolded states.
17. S. H. Park, M. C. R. Shastry, H. Roder, *Nat. Struct. Biol.* **6**, 943 (1999).
18. E. L. McCallister, E. Alm, D. Baker, *Nat. Struct. Biol.* **7**, 669 (2000).
19. A. Morrone *et al.*, *Biophys. J.* **101**, 2053 (2011).
20. B. A. Krantz, L. Mayne, J. Rumbley, S. W. Englander, T. R. Sosnick, *J. Mol. Biol.* **324**, 359 (2002).
21. Clarke and co-workers (*22*) have found, for example, domains with similar structures and stability that have folding rates that differ by ~3000-fold. The slower-folding domains show very little dependence on solvent viscosity, which suggests a large internal friction and, therefore, a much smaller D^* (*22*, *23*).
22. B. G. Wensley *et al.*, *Nature* **463**, 685 (2010).
23. T. Cellmer, E. R. Henry, J. Hofrichter, W. A. Eaton, *Proc. Natl. Acad. Sci. U.S.A.* **105**, 18320 (2008).
24. J. Kubelka, J. Hofrichter, W. A. Eaton, *Curr. Opin. Struct. Biol.* **14**, 76 (2004).
25. R. B. Best, G. Hummer, *Proc. Natl. Acad. Sci. U.S.A.* **102**, 6732 (2005).
26. J. Kubelka, E. R. Henry, T. Cellmer, J. Hofrichter, W. A. Eaton, *Proc. Natl. Acad. Sci. U.S.A.* **105**, 18655 (2008).

Acknowledgments: We thank I. Gopich, A. Szabo, and G. Hummer for numerous helpful discussions and A. Aniana for technical assistance in the expression and purification of proteins. This work was supported by the Intramural Research Program of the National Institute of Diabetes and Digestive and Kidney Diseases, NIH.

Supporting Online Material

www.sciencemag.org/cgi/content/full/335/6071/981/DC1
Materials and Methods
Figs. S1 to S9
Table S1
References (*27–37*)

25 October 2011; accepted 25 January 2012
10.1126/science.1215768

The Alarmin Interleukin-33 Drives Protective Antiviral CD8$^+$ T Cell Responses

Weldy V. Bonilla,[1,2]* Anja Fröhlich,[3,4]* Karin Senn,[5]* Sandra Kallert,[1,2] Marylise Fernandez,[1,2] Susan Johnson,[1,2] Mario Kreutzfeldt,[1,6] Ahmed N. Hegazy,[3,4,7] Christina Schrick,[1,6] Padraic G. Fallon,[8] Roman Klemenz,[5] Susumu Nakae,[9] Heiko Adler,[10] Doron Merkler,[1,6,11] Max Löhning,[3,4]† Daniel D. Pinschewer[1,2]†

Pathogen-associated molecular patterns decisively influence antiviral immune responses, whereas the contribution of endogenous signals of tissue damage, also known as damage-associated molecular patterns or alarmins, remains ill defined. We show that interleukin-33 (IL-33), an alarmin released from necrotic cells, is necessary for potent CD8$^+$ T cell (CTL) responses to replicating, prototypic RNA and DNA viruses in mice. IL-33 signaled through its receptor on activated CTLs, enhanced clonal expansion in a CTL-intrinsic fashion, determined plurifunctional effector cell differentiation, and was necessary for virus control. Moreover, recombinant IL-33 augmented vaccine-induced CTL responses. Radio-resistant cells of the splenic T cell zone produced IL-33, and efficient CTL responses required IL-33 from radio-resistant cells but not from hematopoietic cells. Thus, alarmin release by radio-resistant cells orchestrates protective antiviral CTL responses.

Pathogen-associated molecular patterns (PAMPs) characterize intruding microorganisms and are important for adaptive immune responses to viral infection (*1*). Conversely, endogenous molecular patterns, which indicate tissue injury, are referred to as alarmins and form a second class of damage-associated molecular patterns (DAMPs) (*2*). Unlike PAMPs, the potential contribution of alarmins to antiviral immune defense remains largely elusive.

Many viruses are excellent inducers of cytotoxic CD8$^+$ T lymphocytes (CTLs) (*3*), the basis of which is incompletely understood. To screen

[1]Department of Pathology and Immunology, University of Geneva, 1 rue Michel Servet, 1211 Geneva 4, Switzerland. [2]World Health Organization Collaborating Center for Vaccine Immunology, University of Geneva, Switzerland. [3]Experimental Immunology, Department of Rheumatology and Clinical Immunology, Charité–University Medicine Berlin, Berlin, Germany. [4]German Rheumatism Research Center (DRFZ), a Leibniz Institute, Charitéplatz 1, 10117 Berlin, Germany. [5]Institute for Cancer Research, Department of Pathology, University Hospital of Zurich, Schmelzbergstrasse 12, 8091 Zurich, Switzerland. [6]Division of Clinical Pathology, Geneva University Hospital, 1 rue Michel Servet, 1211 Geneva 4, Switzerland. [7]Department of Gastroenterology, Hepatology and Endocrinology, Campus Charité Mitte, Charité–University Medicine Berlin, Berlin, Germany. [8]Institute of Molecular Medicine, St. James's Hospital, Trinity College Dublin, Dublin 8, Ireland. [9]The Institute of Medical Science, The University of Tokyo, 4-6-1 Shirokanedai, Minato-ku, Tokyo 108-8639, and Japan Science and Technology Agency, Precursory Research for Embryonic Science and Technology (PRESTO), 4-1-8 Hncho, Kawaguchi, Saitama 332-0012, Japan. [10]Helmholtz Zentrum München, Institute of Molecular Immunology and Clinical Cooperation Group Hematopoietic Cell Transplantation (CCG HCT), Marchioninistraße 25, 81377 München, Germany. [11]Department of Neuropathology, University Medical Center, Georg August University, Göttingen, Germany.

*These authors contributed equally to this work.
†These authors contributed equally to this work. To whom correspondence should be addressed. E-mail: loehning@drfz.de (M.L.); daniel.pinschewer@gmx.ch (D.P.P.)

for inflammatory signals augmenting antiviral CTL responses, we used lymphocytic choriomeningitis virus (LCMV) infection of mice. We performed a genome-wide cDNA expression analysis of total spleen tissue from LCMV-infected mice and compared it to an analysis of uninfected controls. From a large panel of interleukins and pro-inflammatory cytokines, interferon-γ (IFN-γ) and IL-33 were most up-regulated (table S1). The IL-33 receptor ST2, an IL-1 receptor family member also known as T1 and IL1RL1, was also up-regulated.

IL-33 is expressed in the nucleus of non-hematopoietic cells, such as fibroblasts and epithelial and endothelial cells of various tissues (*4*), but its role in antiviral CTL responses is unknown. Its bioactive pro-inflammatory form is released as a result of necrosis but not apoptosis, classifying IL-33 as an alarmin (*5*–*7*). IL-33 mRNA expression peaked at 3 to 5 days after infection and grossly paralleled the kinetics of LCMV RNA (Fig. 1A). To test whether IL-33 was important for CTL responses to LCMV, we performed infection experiments in IL-33–deficient ($Il33^{-/-}$) mice (*8*). Absence of IL-33 reduced the absolute number of CTLs responding to the immunodominant LCMV epitope GP33 by >90%. The frequency of epitope-specific CTLs was reduced by >75% (Fig. 1B). When expressed as a nuclear factor in healthy cells, IL-33 is complexed with chromatin and modulates gene expression (*9*). Upon release from necrotic cells, however, IL-33 binds and signals through ST2 (*10*, *11*). To assess which one of these roles of IL-33 accounted for defective CTL responses in $Il33^{-/-}$ mice, we used transgenic mice expressing a soluble decoy receptor for IL-33 [*Il1rl1-Fc* mice (*12*)]. *Il1rl1-Fc* mice displayed defective CTL expansion analogously to $Il33^{-/-}$ mice (fig. S1A). Mice lacking the IL-33 receptor ST2 [$Il1rl1^{-/-}$ (*13*)] also mounted similarly reduced responses to all three LCMV epitopes tested (Fig. 1C and fig. S1, B and C). This indicated that

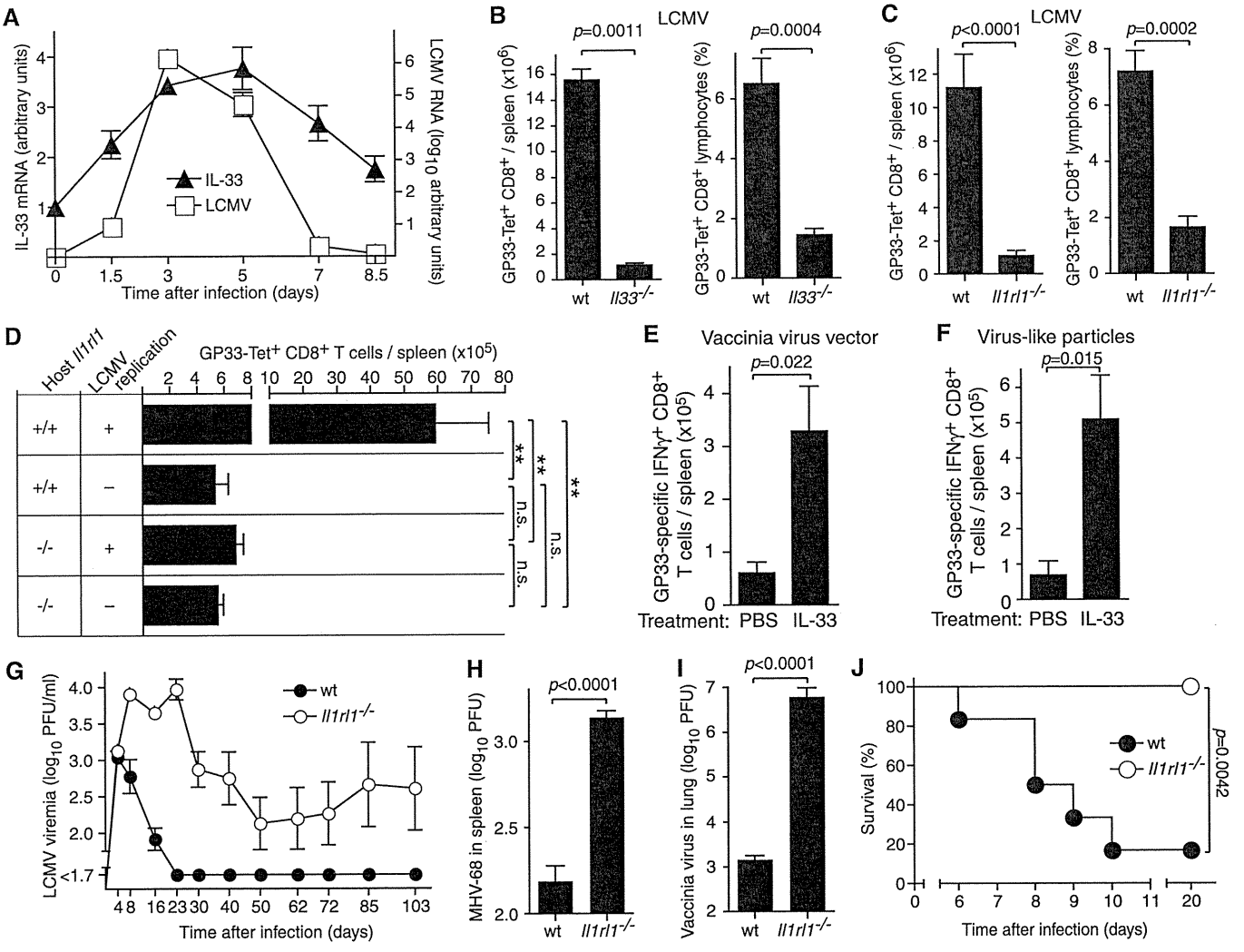

Fig. 1. The IL-33–ST2 pathway drives protective CTL responses to replicating viral infection. (**A**) Kinetic analysis of IL-33 and LCMV RNA expression in the spleen after LCMV infection. Symbols represent the mean ± SEM of four mice. $N = 1$ (N refers to the number of times an experiment was performed). (**B** and **C**) The number of GP33-specific CTLs in the spleen, as detected by peptide–major histocompatibility complex (MHC) tetramer staining, on day 8 after LCMV infection. Bars represent mean ± SEM of five mice. $N = 1$ (B) or 3 (C). (**D**) Epitope-specific CTLs of WT and $Il1rl1^{-/-}$ mice responding to replicating WT LCMV infection or to replication-deficient rLCMV vectors. Bars represent the mean ± SEM of five mice. $N = 2$. $P < 0.0001$ by one-way analysis of variance (ANOVA). Results of Bonferroni's posttest are indicated. n.s., not significant; $^*P < 0.05$; $^{**}P < 0.01$. (**E** and **F**) WT mice were vaccinated with recombinant VV vector expressing LCMV-GP (E) or with GP33-carrying VLPs (F) on day 0 and were treated with IL-33 or diluent [phosphate-buffered saline (PBS)] daily from day 1 to 7, and CTL responses were determined on day 8. Bars represent the mean ± SEM of four to five mice. $N = 2$ (E) or 1 (F). (**G**) Viremia after infection with 2×10^6 plaque-forming units (PFU) of LCMV-WE. Symbols represent the mean ± SEM of five mice. $N = 2$. (**H**) Splenic MHV-68 titers on day 10 after infection. Bars represent the mean ± SEM of five mice. $N = 1$. (**I**) Pulmonary VV titers on day 8 after infection. Bars represent the mean ± SEM of four to five mice. $N = 1$. (**J**) Incidence of choriomeningitis after intracerebral LCMV infection. Terminally diseased animals were killed in accordance with Swiss law. Survival was compared by using the log rank test. Groups of six mice were used. One of two similar experiments is shown. Unpaired two-tailed student's t test was used for statistical analysis in (B), (C), (E), (F), (H), and (I).

IL-33 was released to the extracellular compartment and signaled through ST2 to amplify antiviral CTL responses.

Analogous to the responses against LCMV, an RNA virus, *Il1rl1*$^{-/-}$ mice also exhibited significantly reduced CTL responses against murine γ-herpesvirus 68 [MHV-68 (*14*)], a DNA virus (fig. S1D). In further analogy to LCMV, MHV-68 induced IL-33 mRNA up-regulation (fig. S1E). The differences in CTL responses to LCMV and MHV-68 were also reflected in reduced antigen-specific cytotoxicity (fig. S1, F and G). However, CTL responses to a nonreplicating adenovirus-based vaccine vector were similar in *Il1rl1*$^{-/-}$ and wild-type (WT) mice (fig. S1H).

Given IL-33 can act as an alarmin, we hypothesized that productive viral replication may represent a unifying characteristic of LCMV and MHV-68 infection, differentiating them from adenoviral vectors. Indeed, the CTL responses of WT and *Il1rl1*$^{-/-}$ mice to replication-deficient LCMV-based vaccine vector (*15*) were indistinguishable, and the magnitude of these responses was comparable to the magnitude of responses observed in WT LCMV-infected *Il1rl1*$^{-/-}$ mice (Fig. 1D). Further, *Il1rl1*$^{-/-}$ mice mounted defective CTL responses against WT vaccinia virus (VV), whereas attenuated [thymidine kinase–deficient (*16*)] VV-based vectors induced comparable responses in *Il1rl1*$^{-/-}$ and WT controls (fig. S1I). Thus, we hypothesized that exogenously administered IL-33 could mimic viral replication to enhance vaccine-induced CTL responses. Indeed, recombinant IL-33 significantly augmented CTL responses to VV-based vectors and viruslike particles (VLPs) (Fig. 1, E and F).

CTLs play a pivotal role in the resolution of primary viral infection (*14*, *17*). *Il1rl1*$^{-/-}$ mice controlled low-dose LCMV infection (fig. S1J) but displayed elevated viremia after high-dose LCMV infection and often progressed to viral persistence, whereas WT control mice eliminated the virus (Fig. 1G and fig. S1K). ST2-deficient mice also displayed a log increase in splenic MHV-68 titers and three logs increase in pulmonary VV titers (Fig. 1, H and I). LCMV-neutralizing antibody responses were comparable in *Il1rl1*$^{-/-}$ mice and WT controls (fig. S1L), suggesting that defective CTL responses of *Il1rl1*$^{-/-}$ mice were at the root of impaired LCMV control.

LCMV can cause lethal CTL-mediated immunopathologic disease of the central nervous system when administered intracranially (*17*). Five out of six WT mice developed terminal disease within 10 days, whereas all *Il1rl1*$^{-/-}$ mice survived without clinical signs of immunopathology (Fig. 1J).

The IL-33 receptor ST2 has predominantly been detected on mast cells and CD4$^+$ T helper type 2 cells (*18*–*20*), reportedly exerting pleiotropic effects on helminth-specific immunity, allergy, anaphylaxis, autoimmune, and cardiovascular disease (*20*, *21*). Conversely, ST2 expression on human and mouse CTLs has only recently been found under select in vitro culture and differentiation conditions (*22*). Hence, we investigated which cells were sensing IL-33 for augmenting antiviral CTL responses. To this end, we reconstituted lethally irradiated mice with an approximately 1:1 mixture of WT (CD45.1$^+$) and ST2-deficient bone marrow (CD45.1$^-$) (Fig. 2A and fig. S2A). Compared with uninfected mice, WT cells were 10-fold overrepresented in the population of antigen-specific CTLs responding to LCMV infection (Fig. 2A). In contrast, the repartition of WT and *Il1rl1*$^{-/-}$ B cells remained unaltered (fig. S2A). These observations suggested that virus-reactive

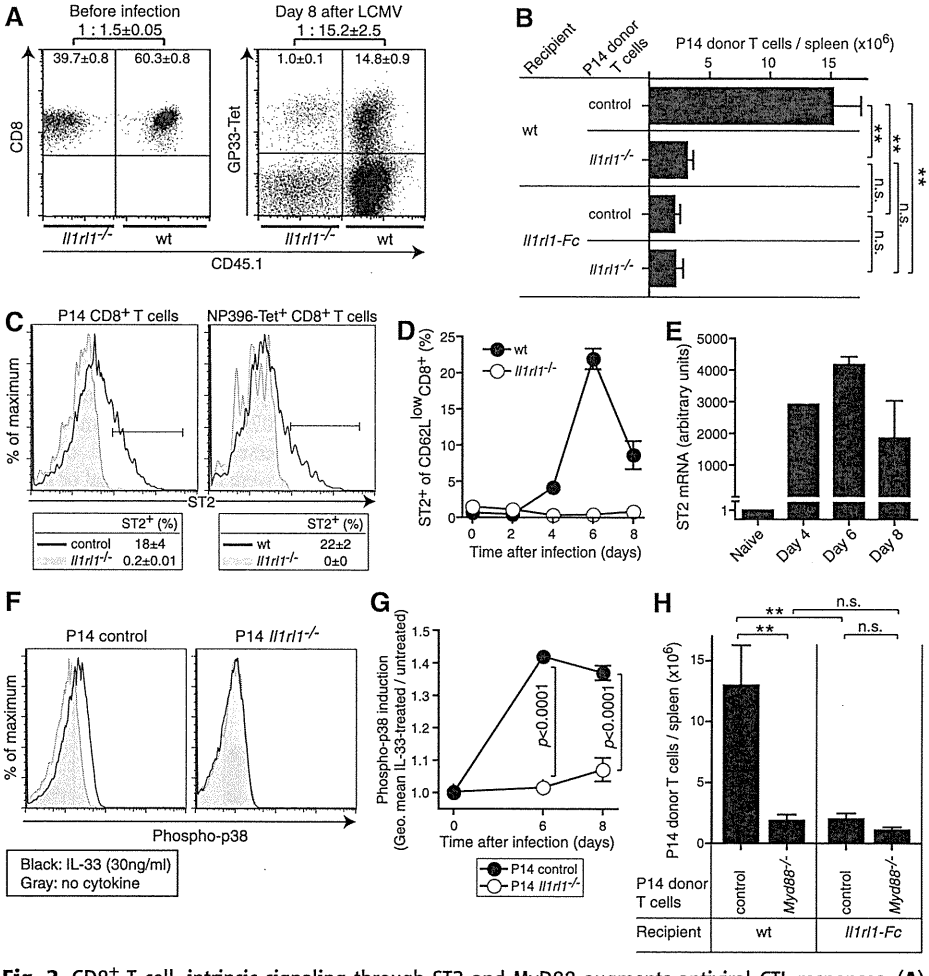

Fig. 2. CD8$^+$ T cell–intrinsic signaling through ST2 and MyD88 augments antiviral CTL responses. (**A**) Irradiated recipients were reconstituted with WT (CD45.1$^+$) and *Il1rl1*$^{-/-}$ (CD45.1$^-$) bone marrow. Flow cytometric analysis of WT and *Il1rl1*$^{-/-}$ total CD8$^+$ T cells before infection (left) and virus-specific CD8$^+$ T cells 8 days after LCMV challenge (right). Values represent mean frequency ± SEM of three mice. $N = 2$. (**B**) Control (CD45.1$^+$CD45.2$^-$) and *Il1rl1*$^{-/-}$ (CD45.1$^+$CD45.2$^+$) P14 CD8$^+$ T cells (10^4) were cotransferred into WT and *Il1rl1-Fc* recipient mice (CD45.1$^-$CD45.2$^+$) and were enumerated on day 8 after LCMV. Bars represent the mean ± SEM of four mice per group. $P < 0.0001$ by one-way ANOVA. Results of Bonferroni's posttest are indicated. One representative of three similar experiments is shown. (**C**) Control and *Il1rl1*$^{-/-}$ P14 cells (10^4) were individually transferred into WT recipients (left). Peptide-MHC tetramer–binding cells in WT and *Il1rl1*$^{-/-}$ mice were studied (right). On day 6 after LCMV infection, the indicated cell populations in spleen were analyzed for ST2 expression by flow cytometry. Values represent the mean ± SD of three mice. $N = 2$. (**D**) Flow cytometric analysis of splenic CD62L^{low}CD8$^+$ T cells over time after LCMV infection. Symbols represent the mean ± SEM of three mice (WT days 2 to 8; *Il1rl1*$^{-/-}$ day 6) or the mean of two mice (other symbols). $N = 2$. (**E**) Quantitative reverse-transcription polymerase chain reaction (qRT-PCR) analysis of ST2 mRNA levels in P14 CD8$^+$ T cells. Day 6 and 8 values represent the mean ± SEM of three mice. RNA samples from three donor mice were pooled for combined analysis on days 0 and 4. $N = 1$. (**F** and **G**) Flow cytometric analysis of intracellular phospho-p38 expression in control and *Il1rl1*$^{-/-}$ P14 cells isolated on day 6 (F) or over time after LCMV infection and treated ex vivo with recombinant IL-33. Symbols in (G) represent the mean ± SEM of three mice. Unpaired two-tailed student's *t* test was used for statistical analysis. One representative of two similar experiments is shown. (**H**) Control (CD45.1$^+$CD45.2$^-$) and *Myd88*$^{-/-}$ (CD45.1$^+$CD45.2$^+$) P14 cells were cotransferred to WT and *Il1rl1-Fc* recipient mice (CD45.1$^-$CD45.2$^+$). Expansion was assessed 8 days after LCMV infection. Bars represent the mean ± SEM of four mice per group. $P = 0.0008$ by one-way ANOVA. Results of Bonferroni's posttest are indicated. $N = 1$.

CTLs respond to IL-33 directly. Independent evidence was obtained when T cell receptor–transgenic GP33-specific CTLs (*23*) (P14 cells) were adoptively transferred, followed by LCMV challenge (Fig. 2B). Impaired expansion of ST2-deficient P14 cells in WT recipients corroborated CTL-intrinsic ST2 signaling. As expected, no such differences were seen between control and ST2-deficient P14 cells in the IL-33–depleted environment of *Il1rl1-Fc* mice (Fig. 2B). Primary CTL responses to LCMV are CD4 T cell independent (*24*), and the differences in CTL responses between WT and *Il1rl1*$^{-/-}$ mice persisted when CD4^{+} T cells were depleted (fig. S2B). Altogether, these findings established a CTL-intrinsic role of ST2 signaling in the expansion of antiviral CTLs.

On day 6 after LCMV infection, we observed ST2 expression on up to 20% of virus-specific CTLs, representing the peak of expression as monitored on activated (CD62L^{low}) CTLs (Fig. 2, C and D, and fig. S2, C and D). In P14 cells, we detected a simultaneous peak of ST2 mRNA (Fig. 2E). IL-33 signaling through ST2 involves the adaptor protein MyD88 and downstream phosphorylation of p38 mitogen-activated protein kinase (*10*). Exposure of day 6 LCMV-infected splenocytes to IL-33 ex vivo increased phospho-p38 levels in control P14 cells but not in ST2-deficient ones (Fig. 2F). In concordance with induction of ST2 expression upon activation, IL-33 failed to trigger detectable phospho-p38 signals in naïve P14 cells but did so on day 6 and 8 after infection (Fig. 2G). MyD88 serves important CTL-intrinsic functions, but the upstream receptor(s) accounting for these effects had remained elusive (*25*). In agreement with previous reports, *Myd88*$^{-/-}$ P14 cells expanded significantly less than control P14 cells when adoptively transferred into WT recipients and challenged with LCMV (Fig. 2H). In the IL-33–depleted environment of *Il1rl1-Fc* recipients, however, control and *Myd88*$^{-/-}$ P14 cells responded equivalently, suggesting that defective expansion of *Myd88*$^{-/-}$ P14 cells was largely attributable to a lack of ST2 downstream signaling.

CTL functionality represents an important correlate of protective capacity (*26*). A substantial proportion of control P14 effector cells were plurifunctional, co-expressing IFN-γ, tumor necrosis factor (TNF)-α, IL-2, and the degranulation marker CD107a in various combinations (Fig. 3A). Conversely, about 95% of ST2-deficient P14 cells were monofunctional or lacked effector function (Fig. 3A). Reduced plurifunctionality was also observed in polyclonal antiviral CTL populations of ST2-deficient compared with WT mice (fig. S3A). Coexpression of granzyme B and CD107a indicates efficient cytotoxicity and was nearly undetectable in ST2-deficient P14 cells (Fig. 3B). Control P14 cells also contained significantly higher levels of the anti-apoptotic protein Bcl-2 than ST2-deficient cells (Fig. 3C).

We performed genome-wide cDNA expression profiling of control and ST2-deficient effector P14 cells, yielding 63 differentially expressed candidate genes (fig. S3B and table S2). We validated differential expression of *Klrb1c* (NK1.1) and *Clec2i*, which influence effector cell differentiation and proliferation (*27*, *28*); *Ifitm1* and *Ifitm3*, which mediate the antiproliferative effects of IFN-γ and pro-apoptotic signals (*29*); and *Tspan5*, which affects cell proliferation, migration, and adhesion (*30*); thus corroborating the broad and profound effects of ST2 signals on the CD8^{+} effector T cell transcriptome (Fig. 3D). The gene that encodes KLRG-1, which is a marker of effector CTLs (*31*), was also among the gene array candidates. Indeed, ST2-deficient P14 cells and virus-specific CTLs of *Il1rl1*$^{-/-}$ mice exhibited a significant reduction in KLRG-1^{high}CD127^{low} effector CTLs, failed to express NK1.1, and expressed somewhat higher levels of the inhibitory receptor PD-1 (Fig. 3, E and F, and fig. S3, C to E). With transition to the memory phase, however, the size of the LCMV-specific CTL pool and the cells' KLRG-1 expression became similar in WT and

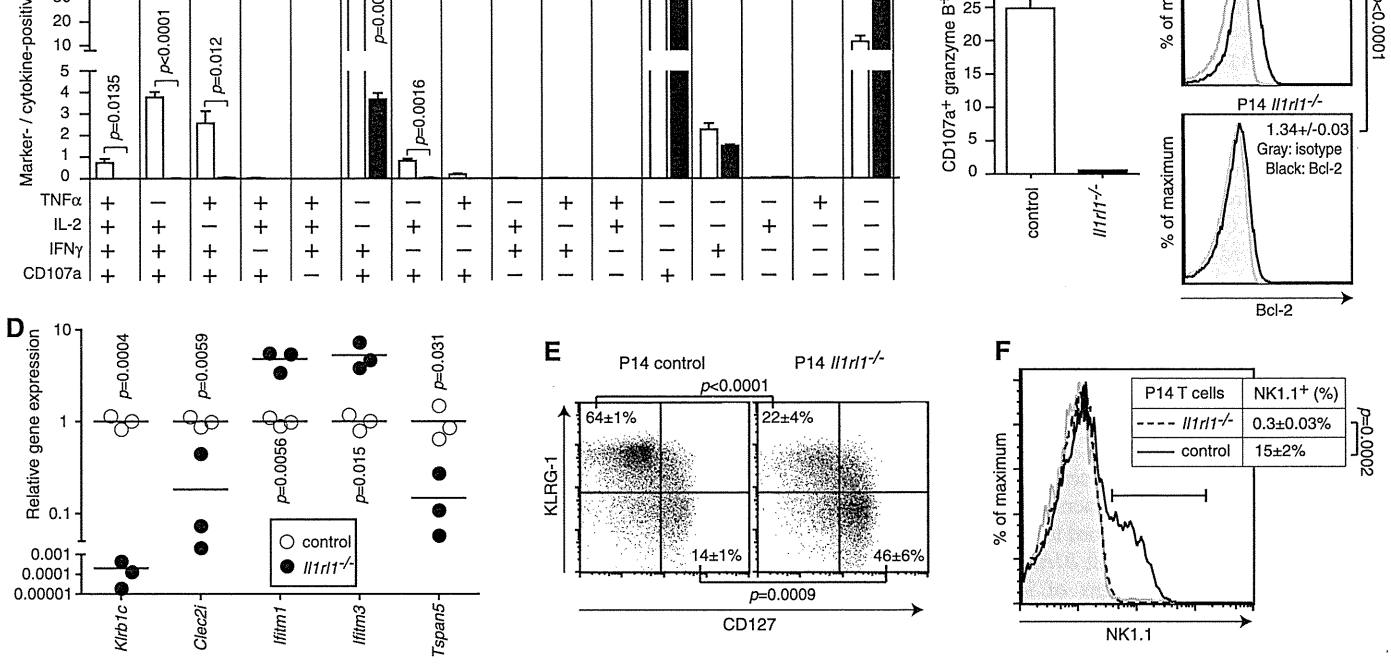

Fig. 3. Broad and profound influence of ST2 signaling on effector CTL differentiation and functionality. (**A** to **C**) CD45.1^{+} control and ST2-deficient P14 CD8^{+} T cells (10^{4}) were adoptively transferred into WT recipient mice, which were then challenged with LCMV. Cytokine profile (A), cytolytic phenotype (B), and Bcl-2 expression (C) were assessed on day 8 after LCMV infection. Bars represent mean ± SEM of three mice. Values in (C) represent geometric mean indices (mean ± SD of three mice per group). $N = 1$ [(A) and (B)] or 2 (C). (**D**) Gene expression profile of P14 cells from recipients as in (A) to (C). The full set of differentially expressed genes is displayed in fig. S3B (also listed in table S2). We validated select genes by qRT-PCR. Symbols show individual mice. $N = 1$. (**E** and **F**) Phenotypic analysis of splenic *Il1rl1*$^{-/-}$ and control P14 CD8^{+} T cells from day 8 LCMV-infected WT recipients as in (A) to (C). Values indicate mean ± SD of three mice. Naïve control P14 T cells are shown as reference in (F) (gray shaded). $N = 1$. Unpaired two-tailed student's t test was used for statistical analysis.

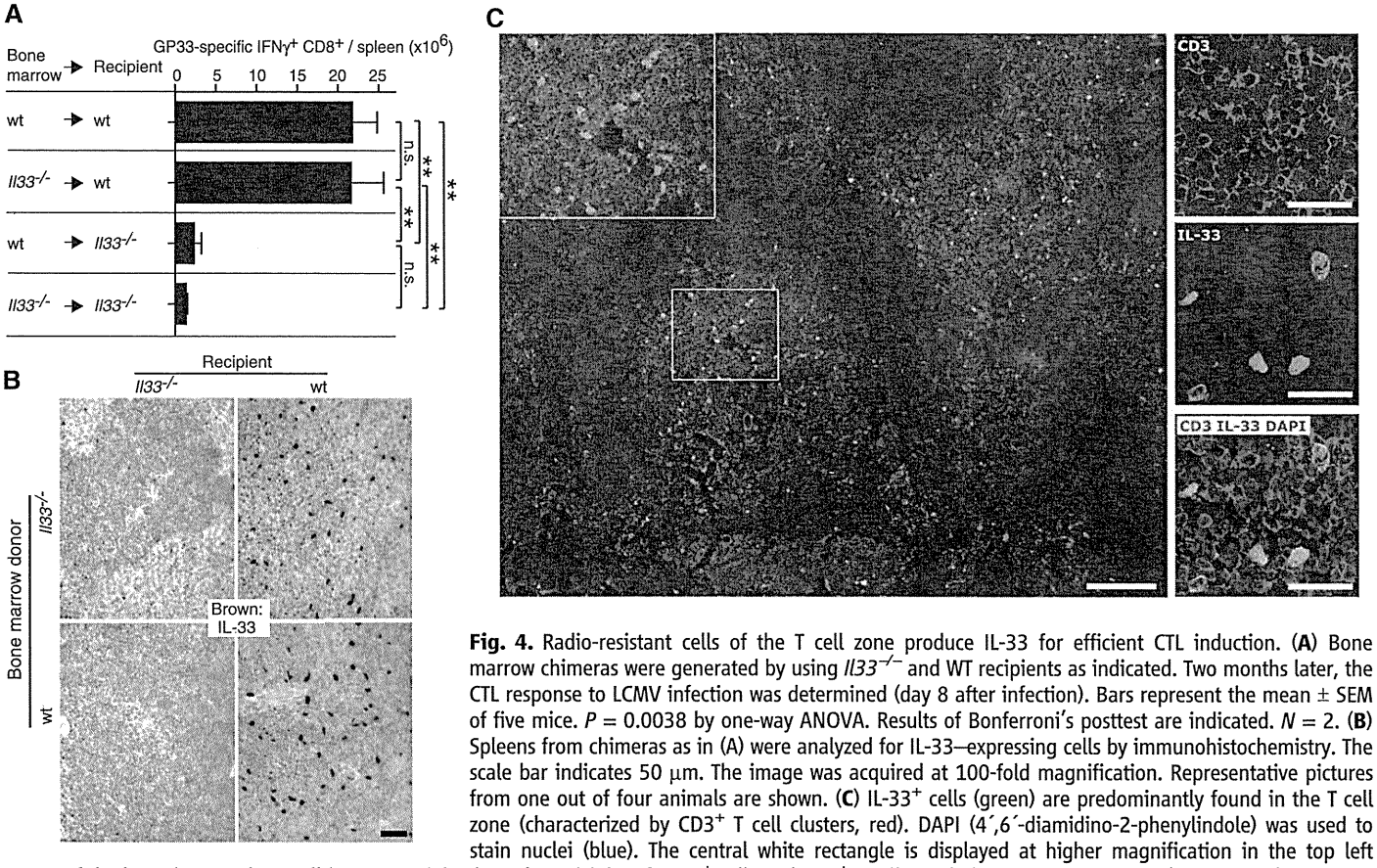

Fig. 4. Radio-resistant cells of the T cell zone produce IL-33 for efficient CTL induction. (**A**) Bone marrow chimeras were generated by using *Il33*$^{-/-}$ and WT recipients as indicated. Two months later, the CTL response to LCMV infection was determined (day 8 after infection). Bars represent the mean ± SEM of five mice. $P = 0.0038$ by one-way ANOVA. Results of Bonferroni's posttest are indicated. $N = 2$. (**B**) Spleens from chimeras as in (A) were analyzed for IL-33–expressing cells by immunohistochemistry. The scale bar indicates 50 μm. The image was acquired at 100-fold magnification. Representative pictures from one out of four animals are shown. (**C**) IL-33^{+} cells (green) are predominantly found in the T cell zone (characterized by CD3^{+} T cell clusters, red). DAPI (4′,6′-diamidino-2-phenylindole) was used to stain nuclei (blue). The central white rectangle is displayed at higher magnification in the top left corner of the large image. The small images at right show close vicinity of IL-33^{+} cells and CD3^{+} T cells. Scale bars indicate 200 μm (large image) or 50 μm (small images and inset). Images were acquired at 200-fold magnification by using a slide scanner (large image and inset) and at 400-fold magnification by confocal microscopy (small images). Representative pictures from one out of four mice are shown.

Il1rl1$^{-/-}$ mice, and vaccinated *Il1rl1*$^{-/-}$ mice controlled LCMV challenge infection as efficiently as WT controls (fig. S3, F and G). This supported the concept that inflammatory signals are more important for primary effector CTL responses than for memory formation (*25*, *32*).

To characterize the cellular source of IL-33 bolstering antiviral CTL responses, we generated reciprocal bone marrow chimeras by using WT or *Il33*$^{-/-}$ mice (Fig. 4A). WT recipient mice generated significantly more LCMV-specific CTLs than *Il33*$^{-/-}$ recipients, irrespective of the IL-33 competence of the bone marrow. These data suggested that radio-resistant, and thus nonhematopoietic, cells are the main source of IL-33. IL-33^{+} cells were only detected in the spleen of chimeras generated from WT recipients, irrespective of the bone marrow received (WT or *Il33*$^{-/-}$, Fig. 4B). IL-33^{+} cells colocalized predominantly with CD3^{+} cells but only sparsely with B cells (Fig. 4C and fig. S4). This was compatible with IL-33 expression by fibroblastic reticular cells (*4*), a stromal cell population of the T cell zone and known target of LCMV infection (*33*).

In light of the evidence for IL-33 to act as an alarmin (*5*, *6*), our findings offer a previously unknown molecular link to understand how viral replication, commonly thought of as "danger" (*34*), can enhance CTL responses to infection. The nonredundancy with PAMPs is noteworthy, particularly in the context of viral replication, which provides abundant PAMP signals (*1*). The observed LCMV dose dependency suggests that the IL-33–ST2 axis is most relevant under conditions of high viral burden. We identified nonhematopoietic cells in the splenic T cell zone expressing IL-33. Depending on the site of initiation and expansion of T cell responses, other cell types expressing IL-33 may also supply this cytokine to CTLs (*35*), and potential regulation by the soluble form of ST2 remains to be investigated (*36*).

PAMPs act primarily on professional antigen-presenting cells and thereby are decisive for efficient priming of CTLs (*37*). IL-33 and possibly also other alarmins have complementary and nonredundant functions and, in the case of IL-33, act on antiviral CTLs directly. Taken together, this study establishes a paradigm for the role of nonhematopoietic cells providing alarmins to augment and differentiate protective CTL responses to viral infection.

References and Notes

1. D. Schenten, R. Medzhitov, *Adv. Immunol.* **109**, 87 (2011).
2. J. J. Oppenheim, D. Yang, *Curr. Opin. Immunol.* **17**, 359 (2005).
3. J. W. Yewdell, S. M. Haeryfar, *Annu. Rev. Immunol.* **23**, 651 (2005).
4. C. Moussion, N. Ortega, J. P. Girard, *PLoS ONE* **3**, e3331 (2008).
5. W. Zhao, Z. Hu, *Cell. Mol. Immunol.* **7**, 260 (2010).
6. G. Haraldsen, J. Balogh, J. Pollheimer, J. Sponheim, A. M. Küchler, *Trends Immunol.* **30**, 227 (2009).
7. C. Cayrol, J. P. Girard, *Proc. Natl. Acad. Sci. U.S.A.* **106**, 9021 (2009).
8. K. Oboki *et al.*, *Proc. Natl. Acad. Sci. U.S.A.* **107**, 18581 (2010).
9. V. Carriere *et al.*, *Proc. Natl. Acad. Sci. U.S.A.* **104**, 282 (2007).
10. J. Schmitz *et al.*, *Immunity* **23**, 479 (2005).
11. C. A. Dinarello, *Annu. Rev. Immunol.* **27**, 519 (2009).
12. K. A. Senn *et al.*, *Eur. J. Immunol.* **30**, 1929 (2000).
13. M. J. Townsend, P. G. Fallon, D. J. Matthews, H. E. Jolin, A. N. McKenzie, *J. Exp. Med.* **191**, 1069 (2000).
14. S. Ehtisham, N. P. Sunil-Chandra, A. A. Nash, *J. Virol.* **67**, 5247 (1993).
15. L. Flatz *et al.*, *Nat. Med.* **16**, 339 (2010).
16. R. M. Buller, G. L. Smith, K. Cremer, A. L. Notkins, B. Moss, *Nature* **317**, 813 (1985).
17. W. P. Fung-Leung, T. M. Kündig, R. M. Zinkernagel, T. W. Mak, *J. Exp. Med.* **174**, 1425 (1991).
18. M. Löhning *et al.*, *Proc. Natl. Acad. Sci. U.S.A.* **95**, 6930 (1998).
19. D. Xu *et al.*, *J. Exp. Med.* **187**, 787 (1998).
20. F. Y. Liew, N. I. Pitman, I. B. McInnes, *Nat. Rev. Immunol.* **10**, 103 (2010).
21. G. Palmer, C. Gabay, *Nat. Rev. Rheumatol.* **7**, 321 (2011).
22. Q. Yang *et al.*, *Eur. J. Immunol.* **41**, 3351 (2011).
23. H. Pircher, K. Bürki, R. Lang, H. Hengartner, R. M. Zinkernagel, *Nature* **342**, 559 (1989).
24. A. Rahemtulla *et al.*, *Nature* **353**, 180 (1991).
25. A. H. Rahman *et al.*, *J. Immunol.* **181**, 3804 (2008).
26. V. Appay, R. A. van Lier, F. Sallusto, M. Roederer, *Cytometry A* **73**, 975 (2008).
27. B. Ljutic *et al.*, *J. Immunol.* **174**, 4789 (2005).

28. W. Tian *et al.*, *Cell. Immunol.* **234**, 39 (2005).
29. M. J. Dobrzanski, J. B. Reome, J. A. Hollenbaugh, R. W. Dutton, *J. Immunol.* **172**, 1380 (2004).
30. L. A. Koopman *et al.*, *J. Exp. Med.* **198**, 1201 (2003).
31. N. S. Joshi *et al.*, *Immunity* **27**, 281 (2007).
32. A. H. Rahman *et al.*, *Blood* **117**, 3123 (2011).
33. S. N. Mueller *et al.*, *Proc. Natl. Acad. Sci. U.S.A.* **104**, 15430 (2007).
34. S. Gallucci, P. Matzinger, *Curr. Opin. Immunol.* **13**, 114 (2001).
35. R. Le Goffic *et al.*, *Am. J. Respir. Cell Mol. Biol.* **45**, 1125 (2011).
36. A. Becerra, R. V. Warke, N. de Bosch, A. L. Rothman, I. Bosch, *Cytokine* **41**, 114 (2008).
37. O. Joffre, M. A. Nolte, R. Spörri, C. Reis e Sousa, *Immunol. Rev.* **227**, 234 (2009).

Acknowledgments: This work was supported by Bundesministerium für Bildung und Forschung (BMBF)–FORSYS (A.F., M.L.), National Health and Medical Research Council (S.J.), German Research Foundation (GRK1121, A.N.H.), Science Foundation Ireland (P.G.F.), Program for Improvement of Research Environment for Young Researchers, the Special Coordination Funds for Promoting Science and Technology from the Japanese Ministry of Education, Culture, Sports, Science and Technology, Japan Science and Technology Agency, PRESTO (S.N.), BMBF (NGFNplus, FKZ PIM-01GS0802-3; H.A.), Wilhelm Sander-Stiftung (H.A.), German Research Foundation (SFB618 and SFB650, M.L.), Volkswagen Foundation (Lichtenberg Program, M.L.), Fondation Leenaards (D.D.P.), European Community (D.D.P.), and Swiss National Science Foundation (D.M., D.D.P.). We thank A. Bergthaler, G. R. Burmester, C. Gabay, M. Geuking, A. Kamath, P. H. Lambert, J. Luban, B. Marsland, G. Palmer, A. Radbruch, C. A. Siegrist, and R. M. Zinkernagel for discussions and advice; H. Saito, National Research Institute for Child Health and Development, for *Il33*$^{-/-}$ mice obtained under a materials transfer agreement (MTA) through the RIKEN Center for Developmental Biology, Laboratory for Animal Resources and Genetic Engineering; A. McKenzie (for *Il1rl1*$^{-/-}$ mice obtained under MTA); the University of Zurich (for rLCMV technology obtained under MTA) and G. Jennings [Cytos Biotechnology AG, Schlieren, Switzerland, holding patent rights on VLPs provided] for reagents; and J. Weber and B. Steer for technical assistance. The data presented in this paper are tabulated in the main paper and the supporting online material. Microarray data are deposited with National Center for Biotechnology Information Gene Expression Omnibus (GEO, accession number GSE34392) and ArrayExpress (accession number E-MTAB-901). D.D.P. is or has been a shareholder, board member, and consultant to ArenaVax AG, Switzerland, and to Hookipa Biotech GmbH, Austria, commercializing rLCMV vectors (patent application EP 07 025 099.8, coauthored by D.D.P.). The authors declare that they do not have other competing financial interests.

Supporting Online Material

www.sciencemag.org/cgi/content/full/science.1215418/DC1
Materials and Methods
Figs. S1 to S4
Tables S1 and S2
References (*38–40*)

18 October 2011; accepted 20 January 2012
Published online 9 February 2012;
10.1126/science.1215418

The Cellular Basis of $GABA_B$-Mediated Interhemispheric Inhibition

Lucy M. Palmer,[1] Jan M. Schulz,[1] Sean C. Murphy,[1] Debora Ledergerber,[1] Masanori Murayama,[2] Matthew E. Larkum[1,3]*

Interhemispheric inhibition is thought to mediate cortical rivalry between the two hemispheres through callosal input. The long-lasting form of this inhibition is believed to operate via γ-aminobutyric acid type B ($GABA_B$) receptors, but the process is poorly understood at the cellular level. We found that the firing of layer 5 pyramidal neurons in rat somatosensory cortex due to contralateral sensory stimulation was inhibited for hundreds of milliseconds when paired with ipsilateral stimulation. The inhibition acted directly on apical dendrites via layer 1 interneurons but was silent in the absence of pyramidal cell firing, relying on metabotropic inhibition of active dendritic currents recruited during neuronal activity. The results not only reveal the microcircuitry underlying interhemispheric inhibition but also demonstrate the importance of active dendritic properties for cortical output.

The connection between the two hemispheres of the cerebral cortex via the corpus callosum is one of the most studied and yet least understood pathways in the brain (*1*, *2*). An important function of transcallosal fibers is to mediate interhemispheric inhibition (*3*, *4*), which influences fine motor control (*5*, *6*), visuospatial attention (*7–9*), and somatosensory processing (*10*, *11*). To investigate the cellular mechanisms of interhemispheric inhibition, we performed in vivo patch-clamp recordings from layer 5 (L5) pyramidal neurons in the hindlimb area of the somatosensory cortex in urethane-anesthetized rats (Fig. 1A). Stimulation of the contralateral hindpaw (contralateral HS) (1-ms duration, 100 V) increased the baseline firing rate by a factor of about 3 (0.9 ± 0.2 to 2.9 ± 0.6 Hz; $P < 0.05$; $n = 19$) (Fig. 1, B to D, black). Ipsilateral hindpaw stimulation (ipsilateral HS), on the other hand, had little influence on the firing rate (1-ms duration, 100V; spontaneous, 1.1 ± 0.2 Hz and evoked, 1.2 ± 0.2 Hz; $n = 19$ (Fig. 1B, green). However, an inhibitory influence of ipsilateral HS could be uncovered by pairing it with contralateral HS (paired HS). Here, paired HS resulted in a significant decrease in evoked firing (evoked, 2.2 ± 0.5 Hz; $n = 19$; $P < 0.05$) when the ipsilateral hindpaw was stimulated 400 ms before the contralateral hindpaw (Fig. 1, B to D, blue). This influence of paired HS on action potential (AP) generation occurred throughout the entire evoked excitatory response, which lasted on average 513 ± 49 ms ($n = 19$) (Fig. 1C, gray area). Unexpectedly, paired HS had no discernible effect on the subthreshold responses (Fig. 1, B to D), which did not significantly decrease in average area (3.4 ± 0.6 versus 3.4 ± 0.6 mV•s; $n = 20$) nor variance (15.7 ± 1.9 versus 17.2 ± 02.1 mV^2; $n = 20$) (fig. S1).

The average 25 ± 8% decrease in the evoked firing during paired HS was somatotopically specific because stimulation of different regions of the body, or even different parts of the hindlimb, did not reduce the response to contralateral HS (fig. S2). Furthermore, the decrease in firing did not occur when the contralateral hindpaw was stimulated twice at an interval of 400 ms (fig. S3), and paired HS had no inhibitory effect on layer 2/3 (L2/3) pyramidal neurons (contralateral HS, 3.9 ± 0.6 Hz; paired HS, 3.6 ± 0.7 Hz; $t = 400$ ms; $n = 9$) (fig. S4). When the timing of the paired-HS interval was varied in 200-ms steps, L5 pyramidal neuron firing was only influenced when the ipsilateral hindpaw was stimulated either 200 or 400 ms before the contralateral hindpaw (Fig. 1E). The long-time course for this type of inhibition suggested the involvement of γ-aminobutyric acid type B ($GABA_B$) receptors, which can exert an effect for up to 500 ms in vitro (*12*). Indeed, application of the $GABA_B$-receptor antagonist, CGP52432 (1 μM) to the cortical surface blocked the decrease in firing generated by paired HS (contralateral HS, 1.9 ± 0.7 Hz; paired HS, 2.0 ± 0.9 Hz, $t = 400$ ms; $n = 8$) (Fig. 1E).

It has been suggested in humans that ipsilateral somatosensory stimulation leads to suppression of sensory responses due to transcallosal inhibition (*13*). We tested this hypothesis in rats using optogenetic stimulation of the transcallosal pathway in vivo. Deep-layer neurons infected with channelrhodopsin-2 (ChR2) conjugated with adenovirus (AAV) sent callosal fibers predominantly to the upper layers of the opposite hemisphere (Fig. 2A and fig. S5) [see supporting online material (SOM)]. Photostimulation (470 nm; trains of 10- by 10-ms pulses at 10 Hz, beginning 400 ms before the sensory stimulus) of callosal input decreased the evoked firing rate of L5 pyramidal neurons by 36 ± 15% when the light was focused above the hemisphere containing the recording electrode ($n = 9$; $P < 0.05$) (Fig. 2, B and C) and by 38% ± 14% with photostimulation of the injected hemisphere ($n = 7$; $P < 0.05$) (fig. S6). Photoactivation of the callosal fibers alone did not influence spontaneous firing activity (0.6 ± 0.2 Hz prephotoactivation and 0.7 ± 0.3 Hz during photoactivation) (fig. S6), and there was

[1]Physiologisches Institut, Universität Bern, Bühlplatz 5, CH-3012 Bern, Switzerland. [2]Behavioral Neurophysiology Laboratory, Brain Science Institute, Riken, 2-1 Hirosawa, Wako, Saitama 351-0198, Japan. [3]Neurocure Cluster of Excellence, Department of Biology, Humboldt University, Charitéplatz 1, 10117, Berlin, Germany.

*To whom correspondence should be addressed. E-mail: matthew.larkum@gmail.com

www.sciencemag.org/cgi/content/full/science.1215418/DC1

Supporting Online Material for

The Alarmin Interleukin-33 Drives Protective Antiviral CD8$^+$ T Cell Responses

Weldy V. Bonilla, Anja Fröhlich, Karin Senn, Sandra Kallert, Marylise Fernandez, Susan Johnson, Mario Kreutzfeldt, Ahmed N. Hegazy, Christina Schrick, Padraic G. Fallon, Roman Klemenz, Susumu Nakae, Heiko Adler, Doron Merkler, Max Löhning,* Daniel D. Pinschewer*

*To whom correspondence should be addressed. E-mail: loehning@drfz.de (M.L.); daniel.pinschewer@gmx.ch (D.P.P.)

Published 9 February 2012 on *Science* Express
DOI: 10.1126/science.1215418

This PDF file includes:

Materials and Methods

Mice and animal experimentation

IL-33$^{-/-}$ mice (*8*) were obtained through the RIKEN Center for Developmental Biology (Acc. No. CDB0631K; http://www.cdb.riken.jp/arg/mutant%20mice%20list.html). *Il1rl1*$^{-/-}$, *Il1rl1-Fc*, P14 and P14 *Myd88*$^{-/-}$ mice have been described (*12, 13, 23, 25*). Animal experiments were performed at the Universities of Geneva and Zurich and at the Charité and German Rheumatism Research Center Berlin in accordance with the Swiss and German laws for animal protection, respectively, and with permission from the local veterinary offices.

Gene expression analysis

Affymetrix GeneChip Mouse Gene 1.0 ST and Applied Biosystems TaqMan RT-PCR assays were utilized for assessing gene expression. TaqMan results were normalized to GAPDH. RNA from FACS-sorted T cells was pre-amplified using the Sigma Aldrich Transplex WTA kit.

Viruses, vaccine vectors and cytokine treatment

LCMV-WE was administered at a dose of 200 PFU intravenously (low dose) unless specified. For intracerebral infection, 10^5 PFU of LCMV Armstrong were given. $2x10^6$ PFU of recombinant (thymidine kinase-deficient) vaccinia virus vector expressing LCMV-GP (*15*) and $4x10^5$ PFU wild type vaccinia virus strain WR were given intravenously. 10^5 PFU of MHV-68 were given intraperitoneally, $3x10^5$ PFU of rLCMV vectors (*15*) were administered intravenously, and vaccination with 200 μg of VLPs carrying GP33 (*39*) was performed

subcutaneously. Infectious LCMV, vaccinia virus and MHV-68 titers, and LCMV RNA were quantified as described (*15, 40*). Recombinant IL-33 (eBioscience, 4 μg per dose) was administered daily intraperitoneally, starting on day 1 after vaccination.

T cell assays, antibody measurements and phospho-p38 MAPK detection

Epitope-specific T cells were enumerated using MHC class I tetramers (Beckman Coulter) and dextramers (Immudex), and by intracellular cytokine assays (*15*). CTL activity was measured in primary ex vivo Cr^{51} release assays. EL-4 cells serving as targets in primary ex vivo CTL assays were loaded with the LCMV-epitope GP33 (KAVYNFATC) or with a mixture of MHV-68 peptides p79 (TSINFVKI) and p56 (AGPHNDMEI). LCMV-neutralizing antibodies were determined in plaque reduction assays (*38*). For FACS detection of phospho-p38 MAPK, cells were serum starved for 5 hours prior to adding recombinant mouse IL-33 (R&D Systems) or mock for 30 min., then were fixed, permeabilized and stained using Phosflow Lyse/Fix buffer, Phosflow perm buffer III and PE anti-phospho-p38 (all from BD Pharmingen). For flow cytometric detection of cell surface ST2, splenocytes were pre-incubated with anti-mouse Fcγ-receptor antibody (clone 2.4G2) followed by staining with digoxigenin-coupled anti-mouse ST2 antibody (clone DJ8, mdbisoscience). For detection, a PE-coupled anti-digoxigenin Fab antibody (Roche) was used. To augment the PE signal we performed two rounds of amplification using the PE FASER Kit (Miltenyi Biotec). As a specificity control for surface ST2 detection by the above procedure (fig. S2C, D), Fc block was washed away, and surface ST2 was blocked by incubation of the splenocytes with uncoupled ST2 antibody (10μg/ml). Subsequently, unbound antibody was washed away and the cells were stained as described above. For detection of surface ST2 on MHC class I tetramer-binding CD8+ T cells, ST2 surface staining and

amplification were performed first, followed by extensive washing with PBS/2% BSA. Only subsequently the splenocytes were incubated with the respective MHC class I tetramer. Further antibodies for flow cytometry were from BD Pharmingen, Biolegend, eBiosciences.

Immunohistochemistry

PFA-fixed tissues were subject to antigen retrieval (microwave), perioxidase inactivation (PBS/3% H_2O_2) and blocked (PBS/10% FCS). Goat anti–mouse IL-33 (R&D Systems), rat anti–human/mouse CD3 (Serotec) and rat anti-mouse/human B220/CD45R (eBioscience) served as primary antibodies and were visualized by an avidin-biotin technique with 3,3′-diaminobenzidine (nuclear haemalaun counterstaining) for light microscopy or with species-specific Alexa555- or Alexa488-conjugated secondary antibodies (Invitrogen) together with DAPI (Sigma-Aldrich) in fluorescence/confocal microscopy.

Bone marrow chimeras and adoptive cell transfer

Recipients of bone marrow ($5x10^6$ cells) were lethally irradiated (11 Gy) the day before transfer, and residual T cells were depleted (100 µg T24 anti-Thy1 antibody intraperitoneally). We purified P14 $CD8^+$ T cells for transfusion (10^4 cells per recipient) by magnetic cell sorting (Miltenyi Biotec).

Statistical analysis

One-way ANOVA with Bonferroni's or Dunnett's post-test were used for multiple comparisons as indicated, unpaired two-tailed student's t test to compare two groups, and logrank tests for

survival curves (Graphpad Prism software vs. 4.0b). $p<0.05$ was considered statistically significant (*), $p<0.01$ as highly significant (**).

Supplementary Table I. Interleukin and inflammatory cytokine expression in LCMV infection

Gene[1]	Gene abbreviation	Genbank reference sequence	Fold change (infected vs. uninfected)	p-value	stepup (p-value)
Interleukins and inflammatory cytokines					
interferon gamma	Ifng	NM_008337	12.47	0.00	0.02
interleukin 33	Il33	NM_001164724	4.60	0.00	0.05
secreted phosphoprotein 1	Spp1	NM_009263	3.65	0.00	0.06
tumor necrosis factor (ligand)	Tnfsf9	NM_009404	3.25	0.02	0.10
interleukin 6	Il6	NM_031168	2.76	0.01	0.08
interleukin 10	Il10	NM_010548	2.54	0.01	0.10
tumor necrosis factor (ligand)	Tnfsf10	NM_009425	2.54	0.00	0.04
interleukin 1 family, member 9	Il1f9	NM_153511	2.15	0.12	0.30
Fas ligand (TNF superfamily, member 6)	Fasl	NM_010177	2.03	0.00	0.03
interleukin 1 alpha	Il1a	NM_010554	1.92	0.00	0.04
growth differentiation factor 15	Gdf15	NM_011819	1.92	0.00	0.05
tumor necrosis factor	Tnf	NM_013693	1.87	0.00	0.04
macrophage migration inhibitory factor	Mif	NM_010798	1.86	0.01	0.08
inhibin beta-A	Inhba	NM_008380	1.86	0.01	0.10
interleukin 1 beta	Il1b	NM_008361	1.85	0.12	0.30
interleukin 21	Il21	NM_021782	1.82	0.01	0.08
interleukin 15	Il15	NM_008357	1.71	0.00	0.04
kit ligand	Kitl	NM_013598	1.36	0.01	0.08
platelet factor 4	Pf4	NM_019932	1.34	0.02	0.12
colony stimulating factor 1 (macrophage)	Csf1	NM_007778	1.32	0.01	0.08
colony stimulating factor 2 (granulocyte-macrophage)	Csf2	NM_009969	1.32	0.02	0.13
tumor necrosis factor (ligand) superfamily, member 14	Tnfsf14	NM_019418	1.29	0.06	0.20
aminoacyl tRNA synthetase complex-interacting multifunctional protein 1	Aimp1	NM_007926	1.25	0.05	0.18
leukemia inhibitory factor	Lif	NM_008501	1.25	0.14	0.33
interleukin 27	Il27	NM_145636	1.18	0.16	0.35
tumor necrosis factor (ligand) superfamily, member 4	Tnfsf4	NM_009452	1.17	0.06	0.20
CD70 antigen	Cd70	NM_011617	1.15	0.15	0.35
tumor necrosis factor (ligand) superfamily, member 8	Tnfsf8	NM_009403	1.12	0.33	0.54
complement component 3	C3	NM_009778	1.12	0.07	0.23
bone morphogenetic protein 5	Bmp5	NM_007555	1.09	0.20	0.40
interferon alpha 2	Ifna2	NM_010503	1.08	0.31	0.52
interleukin 12b	Il12b	NM_008352	1.07	0.59	0.76
tumor necrosis factor (ligand) superfamily, member 11	Tnfsf11	NM_011613	1.07	0.21	0.42
interleukin 23, alpha subunit p19	Il23a	NM_031252	1.04	0.48	0.67
interleukin 17A	Il17a	NM_010552	1.03	0.59	0.76
interleukin 28B	Il28b	NM_177396	1.03	0.70	0.83
interleukin 11	Il11	NM_008350	1.02	0.86	0.93
interleukin 3	Il3	NM_010556	1.02	0.61	0.77
interleukin 24	Il24	NM_053095	1.02	0.79	0.89
bone morphogenetic protein 1	Bmp1	NR_033241	1.01	0.90	0.95
interferon beta 1	Infb1	NM_010510	1.01	0.95	0.98
interleukin 20	Il20	NM_021380	1.00	0.98	0.99
bone morphogenetic protein 8b	Bmp8b	NM_007559	-1.00	1.00	1.00
interleukin 17C	Il17c	NM_145834	-1.01	0.93	0.96
Tnfsf12-tnfsf13 readthrough transcript	Tnfsf12-	NM_001034097	-1.01	0.92	0.96

Tnfsf12-tnfsf13 readthrough transcript	Tnfsf12-Tnfsf13	NM_001034097	-1.01	0.92	0.96
interleukin 1 family, member 6	Il1f6	NM_019450	-1.01	0.84	0.92
interleukin 19	Il19	NM_001009940	-1.01	0.89	0.94
growth differentiation factor 3	Gdf3	NM_008108	-1.01	0.87	0.93
interleukin 4	Il4	NM_021283	-1.01	0.72	0.85
interleukin 1 family, member 8	Il1f8	NM_027163	-1.02	0.93	0.96
myostatin	Mstn	NM_010834	-1.02	0.83	0.91
interferon alpha 4	Ifna4	NM_010504	-1.02	0.72	0.85
interferon alpha 4	Lefty1	NM_010094	-1.03	0.75	0.86
interleukin 34	Il34	NM_029646	-1.03	0.55	0.73
secretoglobin, family 3A, member 1	Scgb3a1	NM_170727	-1.03	0.72	0.85
interleukin 17D	Il17d	NM_145837	-1.03	0.37	0.58
interleukin 5	Il5	NM_010558	-1.03	0.74	0.86
fibroblast growth factor 10	Fgf10	NM_008002	-1.04	0.68	0.82
growth differentiation factor 2	Gdf2	NM_019506	-1.04	0.53	0.72
interleukin 25	Il25	NM_080729	-1.04	0.76	0.87
interleukin 9	Il9	NM_008373	-1.05	0.46	0.66
interleukin 22	Il22	NM_016971	-1.05	0.70	0.83
bone morphogenetic protein 10	Bmp10	NM_009756	-1.06	0.64	0.79
interleukin 17F	Il17f	NM_145856	-1.06	0.65	0.80
tumor necrosis factor (ligand) superfamily, member 18	Tnfsf18	NM_183391	-1.06	0.50	0.69
interferon alpha 1	Ifna1	NM_010502	-1.07	0.14	0.33
interleukin 1 family, member 10	Il1f10	NM_153077	-1.07	0.41	0.61
interleukin 31	Il31	NM_029594	-1.07	0.45	0.65
TNFAIP3 interacting protein 2	Tnip2	NM_139064	-1.07	0.33	0.54
bone morphogenetic protein 7	Bmp7	NM_007557	-1.07	0.23	0.44
interleukin 22	Il22	NM_016971	-1.07	0.61	0.78
interleukin 18	Il18	NM_008360	-1.07	0.63	0.79
interleukin 17B	Il17b	NM_019508	-1.08	0.22	0.43
interleukin 2	Il2	NM_008366	-1.09	0.21	0.42
interleukin 1 family, member 5 (delta)	Il1f5	NM_001146087	-1.09	0.28	0.50
C-reactive protein, pentraxin-related	Crp	NM_007768	-1.09	0.39	0.59
colony stimulating factor 3 (granulocyte)	Csf3	NM_009971	-1.10	0.12	0.30
cardiotrophin 2	Ctf2	NM_198858	-1.10	0.08	0.24
transforming growth factor, beta 1	Tgfb1	NM_011577	-1.10	0.31	0.52
interleukin 13	Il13	NM_008355	-1.12	0.27	0.48
growth differentiation factor 9	Gdf9	NM_008110	-1.13	0.21	0.42
tumor necrosis factor (ligand) superfamily, member 13b	Tnfsf13b	NM_033622	-1.13	0.33	0.54
growth differentiation factor 1	Gdf1	NM_001163282	-1.14	0.20	0.40
bone morphogenetic protein 3	Bmp3	NM_173404	-1.15	0.20	0.41
interleukin 28A	Il28a	NM_001024673	-1.16	0.42	0.63
cardiotrophin 1	Ctf1	NM_007795	-1.17	0.14	0.33
interleukin 12a	Il12a	NM_001159424	-1.19	0.08	0.24
growth differentiation factor 5	Gdf5	NM_008109	-1.22	0.05	0.18
inhibin alpha	Inha	NM_010564	-1.24	0.10	0.27
fibrosin	Fbrs	NM_010183	-1.30	0.01	0.08
interleukin 16	Il16	NM_010551	-1.33	0.00	0.04
bone morphogenetic protein 4	Bmp4	NM_007554	-1.42	0.08	0.24
bone morphogenetic protein 6	Bmp6	NM_007556	-1.46	0.00	0.06

bone morphogenetic protein 2	Bmp2	NM_007553	-1.47	0.02	0.10
growth differentiation factor 11	Gdf11	NM_010272	-1.50	0.01	0.09
lymphotoxin A	Lta	NM_010735	-1.55	0.02	0.10
growth differentiation factor 10	Gdf10	NM_145741	-1.62	0.00	0.06
CD40 ligand	Cd40lg	NM_011616	-1.63	0.01	0.08
FMS-like tyrosine kinase 3 ligand	Flt3l	NM_013520	-1.74	0.00	0.04
interleukin 7	Il7	NM_008371	-1.74	0.00	0.06
lymphotoxin B	Ltb	NM_008518	-1.86	0.01	0.09
Interleukin 33 receptor					
ST2	Il1rl1	NM_001025602	3.07	0.00	0.04

[1] Wt mice were infected with LCMV or were left uninfected (n=3 each), and five days later total spleen RNA was processed for genome-wide cDNA expression analysis. The table displays known interleukins and soluble inflammatory mediators (compiled from the SABiosciences Mouse Inflammatory Cytokines & Receptors PCR Array, SABiosciences Mouse Common Cytokines PCR Array and Lonza Mouse Cytokines and Receptors 96 StellARray qPCR Array) and selectively the IL-33 receptor ST2.

Supplementary Table II. Differentially expressed genes in wt and *Il1rl1*$^{-/-}$ effector CTLs

Gene[1]	Gene abbreviation	Genbank reference sequence	Fold difference (*Il1rl1*$^{-/-}$ vs. wt)	p-value	stepup (p-value)
RIKEN cDNA I830127L07 gene	I830127L07Rik	XM_001477102	0.06	0.00	0.00
killer cell lectin-like receptor subfamily B member 1C	Klrb1c	NM_008527	0.11	0.00	0.00
small nucleolar RNA, C/D box 34	Snord34	NR_002455	0.16	0.00	0.00
small nucleolar RNA, C/D box 32A	Snord32a	NR_000002	0.18	0.00	0.00
thymine DNA glycosylase	Tdg	NM_011561	0.23	0.00	0.02
small nucleolar RNA, C/D box 61	Snord61	NR_002903	0.24	0.00	0.01
small nucleolar RNA, C/D box 35A	Snord35a	NR_000003	0.27	0.00	0.00
MRT4, mRNA turnover 4, homolog (S. cerevisiae)	Mrto4	NM_023536	0.31	0.00	0.03
small nucleolar RNA, C/D box 82	Snord82	NR_002851	0.34	0.00	0.00
predicted gene, ENSMUSG00000053178	ENSMUSG00000053178	NM_001042670	0.38	0.00	0.01
tetraspanin 5	Tspan5	NM_019571	0.40	0.00	0.00
killer cell lectin-like receptor subfamily G, member 1	Klrg1	NM_016970	0.40	0.00	0.02
C-type lectin domain family 2, member i	Clec2i	NM_020257	0.41	0.00	0.00
histone cluster 1, H1c	Hist1h1c	NM_015786	0.43	0.00	0.02
coiled-coil-helix-coiled-coil-helix domain containing 2	Chchd2	NM_024166	0.46	0.00	0.03
myeloid-associated differentiation marker	Myadm	NM_001093764	0.47	0.00	0.01
beta-gamma crystallin domain containing 3	Crybg3	NM_174848	0.47	0.00	0.00
RIKEN cDNA 5830405N20 gene	5830405N20Rik	NM_183264	0.48	0.00	0.01
arsenic (+3 oxidation state) methyltransferase	As3mt	NM_020577	0.48	0.00	0.01
hypothetical protein LOC100039226	LOC100039226	XM_001472441	0.48	0.00	0.01
MHC class Ib T9	H2-t9	XR_034252	0.48	0.00	0.03
myc induced nuclear antigen	Mina	NM_025910	0.49	0.00	0.00
predicted gene, EG630061	EG630061	NA	0.49	0.00	0.01
predicted gene, EG666180	EG666180	XR_032038	0.49	0.00	0.03
histone cluster 1, H4b	Hist1h4b	NM_178193	2.00	0.00	0.00
serine (or cysteine) peptidase inhibitor, clade A, member 3F	Serpina3f	NM_001033335	2.02	0.00	0.02
ubiquinol-cytochrome c reductase hinge protein	Uqcrh	NM_025641	2.02	0.00	0.03
predicted gene, EG433216	EG433216	XM_484764	2.03	0.00	0.00
predicted gene, OTTMUSG00000011028	OTTMUSG00000011028	XR_033026	2.04	0.00	0.00
minichromosome maintenance deficient 3 (S. cerevisiae)	Mcm3	NM_008563	2.04	0.00	0.00
zinc finger CCCH-type containing 4	Zc3h4	NM_198631	2.05	0.00	0.00
histone cluster 4, H4	Hist4h4	NM_175652	2.06	0.00	0.00
histone cluster 1, H1a	Hist1h1a	NM_030609	2.07	0.00	0.00
bolA-like 2 (E. coli)	Bola2	NM_175103	2.07	0.00	0.00
gene model 1943, (NCBI)	Gm1943	NR_002928	2.08	0.00	0.01
adhesion molecule, interacts with CXADR antigen 1	Amica1	NM_001005421	2.11	0.00	0.00
predicted gene, EG666487	EG666487	XM_984165	2.12	0.00	0.00
predicted gene, EG665395	EG665395	XM_976637	2.12	0.00	0.00
predicted gene, EG632013	EG632013	XM_001476014	2.15	0.00	0.00
interferon, alpha-inducible protein 27 like 2A	Ifi27l2a	NM_029803	2.16	0.00	0.01
interferon induced transmembrane protein 2	Ifitm2	NM_030694	2.17	0.00	0.04
calmodulin 3	Calm3	NM_007590	2.19	0.00	0.00
predicted gene, EG620161	EG620161	XM_884551	2.21	0.00	0.01
cytochrome c oxidase, subunit XVII assembly protein homolog (yeast)	Cox17	NM_001017429	2.25	0.00	0.01
predicted gene, 631266	631266	XR_031115	2.26	0.00	0.00
coiled-coil domain containing 72	Ccdc72	NM_183250	2.28	0.00	0.04
predicted gene, ENSMUSG00000043424	ENSMUSG00000043424		2.28	0.00	0.00
SPC24, NDC80 kinetochore complex component, homolog (S. cerevisiae)	Spc24	XM_001479281	2.29	0.00	0.00
histone cluster 1, H1b	Hist1h1b	NM_020034	2.32	0.00	0.00

predicted gene, EG621983	EG621983	XR_031283	2.35	0.00	0.00
glucosaminyl (N-acetyl) transferase 1, core 2	Gcnt1	NM_001136484	2.35	0.00	0.03
predicted gene, 100042266	100042266	XR_033208	2.39	0.00	0.02
phytanoyl-CoA hydroxylase	Phyh	NM_010726	2.44	0.00	0.00
similar to ribosomal protein L21	LOC100043646	XM_001480428	2.46	0.00	0.01
ubiquitin-conjugating enzyme E2C	Ube2c	NM_026785	2.51	0.00	0.01
serine carboxypeptidase 1	Scpep1	NM_029023	2.61	0.00	0.00
capping protein (actin filament), gelsolin-like	Capg	NM_001042534	2.72	0.00	0.00
histone cluster 1, H2bj	Hist1h2bj	NM_178198	2.76	0.00	0.00
predicted gene, EG268988	EG268988	XR_030883	2.83	0.00	0.02
predicted gene, OTTMUSG00000001052	OTTMUSG00000001052	XR_032685	2.90	0.00	0.00
lymphocyte antigen 6 complex, locus C1	Ly6c1	NM_010741	3.58	0.00	0.00
interferon induced transmembrane protein 1	Ifitm1	NM_001112715	3.84	0.00	0.00
interferon induced transmembrane protein 3	Ifitm3	NM_025378	5.09	0.00	0.00
serine (or cysteine) peptidase inhibitor, clade A, member 3G	Serpina3g	NM_009251	5.32	0.00	0.00

[1] $CD45.1^+$ control and *Il1rl1*$^{-/-}$ P14 indicator CD8 T cells (10^4) were transferred to separate groups of wt recipient mice and were challenged with LCMV. Eight days later, LCMV-specific $CD45.1^+$ $CD8^+$ indicator CTLs were sorted by flow cytometry and were processed for genome-wide cDNA expression analysis (n=3 for each group). Genes are displayed, which were ≥2-fold differentially expressed, with a step-up p-value of <0.05.

Supporting figure legends

Fig. S1. IL-33 drives protective CTL responses to replicating viral infection, is induced by MHV-68, and is necessary for control of high dose but not low dose LCMV infection.
A-D: Splenic LCMV-specific CTLs on day 8 (A-C) and MHV-68-specific CTLs (D) on day 10 after infection. Bars represent the mean±SEM of five (A-C) or four (D) mice. One out of two similar experiments is shown in A and B. *N*=1 for C-D. E: Kinetic analysis of IL-33 mRNA expression in the spleen after MHV-68 infection. Symbols represent the mean±SEM of four mice. $P<0.0001$ by 1-way ANOVA. Results of Dunnett's post-test comparing against day 0 values are indicated. n.s.: not significant ; *: $p<0.05$; **: $p<0.01$. *N*=1. F-G: Splenocytes as in A-D were tested in primary ex vivo Cr51 release assays. *N*=2 (F) or 1 (G). H-I: CTL response to replication-defective adenoviral vector expressing GP33 (H) and wt vaccinia virus or recombinant vaccinia virus vector expressing LCMV-GP (I). Bars represent the mean±SEM of three to five mice. One representative of two similar experiments is shown. J: LCMV titers in spleen after infection with 200 PFU (standard low dose) of LCMV-WE. Symbols represent the mean of two to six mice per time point. Data are combined from three experiments. K: Viremia after infection with $2x10^6$ PFU of LCMV Clone 13. Symbols represent the mean±SEM of four to six mice. *N*=1. L: LCMV-neutralizing antibody in serum after infection with $2x10^6$ PFU of LCMV-WE (high dose, same experiment as in Fig. 1G) as determined in plaque reduction assays (*38*). Symbols represent the mean±SEM of four to five mice. One representative of two similar experiments is shown. The *p*-values displayed in the figures were obtained using unpaired two-tailed student's t test.